

UNCLASSIFIED

AD NUMBER

AD839744

LIMITATION CHANGES

TO:

Approved for public release; distribution is unlimited.

FROM:

Distribution authorized to U.S. Gov't. agencies and their contractors;
Administrative/Operational Use; SEP 1968. Other requests shall be referred to Commander, Arnold Engineering Development Center, Attn: AETS.
Arnold Air Force Base, TN 37389.

AUTHORITY

AEDC ltr 21 Apr 1972

THIS PAGE IS UNCLASSIFIED

AEDC-TR-68-112

W. E. BLORE

Unclassified

**OBSERVATIONS OF SPHERE WAKES OVER A WIDE RANGE
OF VELOCITIES AND AMBIENT PRESSURES**



A. B. Bailey

ARO, Inc.

September 1968

This document is subject to special export controls and each transmittal to foreign governments or foreign nationals may be made only with prior approval of Arnold Engineering Development Center (AEDC), Arnold Air Force Station, Tennessee 37389.



DOC NUM SER CN

**VON KÁRMÁN GAS DYNAMICS FACILITY
ARNOLD ENGINEERING DEVELOPMENT CENTER
AIR FORCE SYSTEMS COMMAND
ARNOLD AIR FORCE STATION, TENNESSEE**

Unclassified

NOTICES

When U. S. Government drawings specifications, or other data are used for any purpose other than a definitely related Government procurement operation, the Government thereby incurs no responsibility nor any obligation whatsoever, and the fact that the Government may have formulated, furnished, or in any way supplied the said drawings, specifications, or other data, is not to be regarded by implication or otherwise, or in any manner licensing the holder or any other person or corporation, or conveying any rights or permission to manufacture, use, or sell any patented invention that may in any way be related thereto.

Qualified users may obtain copies of this report from the Defense Documentation Center.

References to named commercial products in this report are not to be considered in any sense as an endorsement of the product by the United States Air Force or the Government.

OBSERVATIONS OF SPHERE WAKES OVER A WIDE RANGE
OF VELOCITIES AND AMBIENT PRESSURES

A. B. Bailey
ARO, Inc.

This document is subject to special export controls and each transmittal to foreign governments or foreign nationals may be made only with prior approval of Arnold Engineering Development Center (AEDC), Arnold Air Force Station, Tennessee 37389.

FOREWORD

The research reported herein was sponsored by the Arnold Engineering Development Center (AEDC), Air Force Systems Command (AFSC), under Program Element 6240533F, Project 8952.

The results of the research presented herein were obtained by ARO, Inc. (a subsidiary of Sverdrup & Parcel and Associates, Inc.), contract operator of AEDC, AFSC, Arnold Air Force Station, Tennessee, under contract F40600-69-C-0001. The experimental data were obtained between January 1965 and March 1968 under ARO Project No. VK3080, VT2629, VG2706, VT2711, and VT0878. The manuscript was submitted for publication on April 24, 1968.

The author would like to express his appreciation to O. H. Bock for the design, development, and operation of the schlieren systems used in this study and for the many helpful discussions related to the interpretation of the flow field photographs. The incompressible wake photographs were obtained by K. E. Koch.

Information in this report is embargoed under the Department of State International Traffic in Arms Regulations. This report may be released to foreign governments by departments or agencies of the U. S. Government subject to approval of the Arnold Engineering Development Center (AETS), or higher authority within the Department of the Air Force. Private individuals or firms require a Department of State export license.

This technical report has been reviewed and is approved.

Eugene C. Fletcher
Lt Colonel, USAF
AF Representative, VKF
Directorate of Test

Roy R. Croy, Jr.
Colonel, USAF
Director of Test

ABSTRACT

The behavior of the near and far wake of spheres for a wide range of velocities, $4000 \leq V_\infty \leq 23,000$ ft/sec, and ambient pressures, $10 \leq p_\infty \leq 730$ mm Hg, has been studied with schlieren techniques in an aeroballistic free-flight range. In the present report, attention is drawn to some of the problems of interpreting photographs of this type. It is shown that the mode of operation of the schlieren system, e. g., vertical or horizontal knife edge, can exercise a profound effect on the aspects of the flow that are visualized. The breakthrough phenomenon, which has been considered to exist only at near reentry velocities, is shown to exist at lower supersonic speeds. Schlieren photographs of the far wake of hypersonic spheres in the Reynolds number range of $3 \times 10^4 \leq Re_\infty \leq 8 \times 10^4$ bear a marked resemblance to photographs of the wake of a subsonic bluff body. For both hypersonic and subsonic cases, this photographic evidence indicates the existence of a large-scale vortex structure in the wake.

This document is subject to special export controls and each transmittal to foreign governments or foreign nationals may be made only with prior approval of Arnold Engineering Development Center (AETS), Arnold Air Force Station, Tennessee 37389.

CONTENTS

	<u>Page</u>
ABSTRACT	iii
NOMENCLATURE	vi
I. INTRODUCTION	1
II. APPARATUS	2
III. DISCUSSION OF RESULTS	
3.1 Survey of Wake Transition and Breakthrough Phenomena	3
3.2 Inviscid Wake	4
3.3 Breakthrough	8
3.4 Low Reynolds Number Wake	10
IV. CONCLUSIONS	13
REFERENCES	14

APPENDIX Illustrations

Figure

1. Flow Field of a Hypersonic Sphere	19
2. Single-Pass Schlieren System.	20
3. Expected Location of Inviscid Breakup and Turbulence Breakthrough (Attributable to Wilson, Ref. 2)	21
4. Flow Field of a Supersonic Sphere.	23
5. Wake Flow Field of a Sphere at Low Hypersonic Speeds	25
6. Variation of Inviscid Wake Diameter with Velocity for Spheres	35
7. Sphere Wake at Low Speed and Low Ambient Pressure.	36
8. High-Speed Sphere Wake	39
9. High-Speed Breakthrough.	43
10. High-Speed Turbulent Wake.	45
11. Sphere Wake Diameter.	49
12. Wake Characteristics at Low Reynolds Number	51

<u>Figure</u>	<u>Page</u>
13. Laminar Wake Breakup of a Hypersonic Slender Cone	53
14. Wake Characteristics at Low Reynolds Number	54
15. Incompressible Wake of Bluff Body	59
16. Far Wake Characteristics for Various Model Materials	61
17. High-Speed, Low Reynolds Number Sphere Wake	65

NOMENCLATURE

- D Model diameter
- M_∞ Free-stream Mach number
- p_∞ Free-stream pressure
- Re_∞ Free-stream Reynolds number based on diameter, D
- V_∞ Free-stream velocity
- x Axial distance

SECTION I INTRODUCTION

The wakes generated by high-speed bodies have been studied for the past several years (Refs. 1 through 12). It has been shown that the character of a body wake is a function of (among other parameters), body shape, size, ambient pressure, and velocity. This dependence has resulted in the wake being considered as a source of observables, which, if interpreted correctly, can be used to deduce the size and shape of the body. At this time, the backscattered radar signals from the wakes of full-scale bodies provide one of the main sources of information. The interaction of an electromagnetic wave with an ionized trail can be shown to be dependent on the electron density, collision frequency, wake width, and the laminar or turbulent nature of the flow. The electrical properties of the wake can be strongly affected by the presence of foreign gases in the wake. Such gases can, depending on their composition, either increase or decrease the wake electron density level and decay rate.

It has been suggested (Ref. 1) that a sphere traveling at hypersonic speeds is characterized by the following flow regimes (Fig. 1, Appendix):

1. The almost normal detached bow shock wave in the stagnation region of the body,
2. An essentially inviscid, high-temperature outer wake composed of gas which has passed through the strong, curved portion of the bow shock, and
3. The viscous, high-temperature inner wake generated by the body boundary layer.

To these three main regions must be added the wake shock formed at the wake neck behind the body, the separation shock originating at the body shoulder, and the slip boundary originating at the intersection of these two shock waves.

Goldburg (Ref. 9) considers items 2 and 3 to be not fully descriptive of the flow field of a hypersonic sphere. Goldburg also considers more descriptive and accurate designations to be shock- and boundary-layer-induced wakes. Although there may be a lack in rigor in items 2 and 3, this nomenclature will be adhered to in the present report since the terms are now in common usage.

Investigations of the laminar to turbulent wake transition phenomenon have been made in aeroballistic ranges using schlieren techniques

(Refs. 1 through 6) and oblique doppler radar techniques (Refs. 8 and 10). At low speeds no problems appear to have been encountered in defining the onset of turbulence using schlieren techniques. At higher speeds the inviscid wake appears to have exercised a marked shielding effect on inner wake flow details to be visualized. The backscattered return obtained with a 35-gHz oblique doppler radar system undergoes a noticeable change when the flow changes from laminar to turbulent for ablating and nonablating spheres (Refs. 8 and 10).

As a result of extensive studies (Ref. 2) of hypersonic sphere viscous and inviscid wakes, it has been shown that the region where the viscous inner wake has expanded to such a size that it totally engulfs the inviscid wake and becomes visible in a schlieren photograph is a function of ambient pressure and velocity. Radar and radiation signals from the wake (Refs. 11 and 12) appear to confirm that this phenomenon, called "breakthrough," is a detectable event with these systems also.

The purpose of the present report is to present a series of schlieren photographs and related conclusions with regard to subscale measurements of transition, breakthrough, and inviscid wake breakup behind spheres.

SECTION II APPARATUS

The experimental results discussed in this report have been obtained in the 100-ft hypervelocity pilot range (Armament Test Cell, Hyperballistic (K)) and the 1000-ft hypervelocity range (Armament Test Cell, Hyperballistic (G)). These ranges are fully described in Ref. 13. Various two-stage light-gas guns have been used to launch models in each of these ranges. In the present series of tests, spheres made from nylon, aluminum, tungsten carbide, copper, and steel have been launched at speeds up to 23,500 ft/sec in the ambient pressure range from 10 to 730 mm Hg. It can be assumed that for some of these models and flight conditions, model ablation does occur.

In Ranges K and G, there is a single-pass quasi-parallel-light schlieren system having 12- and 30-in. -diam fields of view, respectively. A schematic of the main components comprising each of these systems is shown in Fig. 2. It is possible to operate either of these systems in the following modes: vertical or horizontal knife edge, Wollaston prism and color grating, or as a focused shadowgraph. For single-flash operation a Speed Graphic® camera is usually used. The

multispark Strobokin[®] light source is used in conjunction with a high-speed drum camera. As many as 20 photographs of the wake can be obtained with this mode of operation. A 35-mm Fastax[®] camera with a framing rate up to 5000 frames/sec can be used for studies of the far wake. It must be realized that both of these multiframe modes of operation result in a loss of definition when compared with single-frame mode of operation. However, in studies involving the far wake, this loss in definition is more than compensated for by the large number of wake photographs.

At low ambient pressures the maximum sensitivity of the single-pass schlieren system can only be achieved when an opaque knife edge is used. This mode of operation also requires a considerable degree of stability in the schlieren support structure. In Range G the schlieren support system has great stability, and problems of system vibration even at the highest sensitivity are rarely encountered. In the design of the Range K system, spatial limitations and the presence of some large rotary equipment made it impossible to arrive at a completely satisfactory support system. To offset to some extent the support system inadequacies, O. H. Bock of this facility has designed a servocontrolled knife-edge system which permits operation at high sensitivities in the presence of system vibration.

At high ambient pressures the Fresnel lens shadowgraph systems described in Ref. 13 provide an adequate visualization of the sphere wake.

SECTION III DISCUSSION OF RESULTS

3.1 SURVEY OF WAKE TRANSITION AND BREAKTHROUGH PHENOMENA

To place the problem to be discussed in perspective, some of the observations that have been made with regard to these events will be briefly summarized. Wilson, Ref. 2, has concluded that (1) the inviscid wake will only be visualized by a schlieren system when the body is at or near reentry velocities (i. e., on the order of 20,000 fps), (2) at low supersonic speeds this inviscid wake will be too weak to be visualized by a schlieren system, and (3) at subsonic speeds an inviscid wake cannot exist because there is no bow shock wave. It has been concluded that there are three Reynolds number regimes of interest (Fig. 3):

1. High Reynolds number where transition in the viscous wake occurs close to the body and the turbulent wake grows rapidly and engulfs the inviscid wake,
2. Intermediate Reynolds number where transition in the inner viscous wake occurs further from the body and there is a rearward shift of the point of breakthrough, and
3. Low Reynolds number where, as has been predicted by Lees (Ref. 14), transition in the viscous inner wake does not occur.

However, far enough behind the body, the inviscid wake also may become unstable and subsequently turbulent. This suggests that at the low Reynolds numbers necessary to suppress viscous wake growth and transition to great enough distance behind the body, the so-called inviscid wake may exhibit "viscous" effects. It is this apparent contradiction that led Goldburg (Ref. 9) to seek a more accurate description of the inviscid wake, which, as we all recognize, is not really inviscid at all.

There appears to be a considerable degree of arbitrariness in the designation of actual Reynolds numbers that delineate the bounds of these three flow regimes. Wilson (Ref. 2) shows photographs of these three types of flow. In one case Wilson shows a typical high Reynolds number example of breakthrough. In another case he shows a typical example of inviscid wake breakup, usually considered a low Reynolds number event. For both of these examples the Reynolds number was equal to approximately 2.5×10^5 .

3.2 INVISCID WAKE

As has been noted earlier, the concept of an inviscid wake [as observed with a horizontal (or oriented in the flight direction) knife-edge schlieren system] is applicable to bodies traveling at or near reentry velocities ($V_\infty \geq 19,000$ ft/sec). In the light of this conclusion let us consider the flow field of a supersonic sphere as shown in Fig. 4. The orthogonal Fresnel lens shadowgrams clearly show a turbulent inner wake close to the body. Superposed on this small-scale turbulence there are some relatively large undulations in the wake flow. In the color print obtained with a horizontal color grating, the small-scale turbulence of the inner wake is not well defined. However, the definition is good enough for it to be concluded that the inner wake is turbulent. The turbulent inner wake details are shielded by what can only be called an inviscid wake. The existence of an "inviscid" wake in this case is at variance with the view that it is a hypersonic phenomenon because velocity in this case was below 4000 fps.

A review of the literature concerning sphere wakes reveals data confirming the existence of an apparent inviscid wake at less than re-entry velocities. Birkhoff, Eckerman, and McKay in Ref. 5 present a sequence of sphere wake photographs where they state, "In the first frame only an (apparently laminar) inviscid wake is visible; there is not enough density change to make the inner core visible. By frame two, the outer edges of the turbulent inner core are visible. In frame three, the entire wake has become visibly turbulent and the inviscid wake is turbulent." This statement pertained to a 0.42-in. -diam sphere at range pressure of 200 mm Hg and a velocity of 14,000 ft/sec. An apparent inviscid wake also is shown to exist for flight conditions of $10,900 \leq V_{\infty} \leq 13,500$ ft/sec and $100 \leq p_{\infty} \leq 300$ mm Hg in Ref. 6. Some wake photographs illustrating this apparent inviscid wake for these flight conditions are shown in Fig. 5.

Figure 5a consists of a sequence of wake photographs obtained with the multispark drum camera system at a velocity of 10,900 ft/sec using a horizontal Wollaston prism. The apparent inviscid wake is clearly identified, as is the region where the turbulent wake engulfs this boundary. It is not possible to determine whether the inner wake is turbulent when it is totally enclosed by the inviscid wake. A series of single-spark photographs, Figs. 5b and c, obtained at higher speed and pressure show clearly that the inner wake is turbulent within this boundary.

Figure 5d presents a sequence of wake photographs obtained with a vertical Wollaston prism. The model flight conditions are similar to those quoted in Fig. 5a. Although the inner wake is observed to some extent in the early frames of this sequence (Fig. 5d), as would be expected with the vertical prism orientation, no clearly identifiable inviscid wake can be seen.

A shadowgram of a sphere wake is shown in Fig. 5e. A detailed study of this photograph indicates the existence of a series of weak shocks which appears to originate at the turbulent wake edge. These weak waves appear to terminate on a boundary parallel to the flight direction. To focus attention on these weak waves a portion of this boundary has been accentuated in Fig. 5e.

Another shadowgram is shown in Fig. 5f. A study of this photograph reveals a turbulent wake close to the neck. The wake is not visible downstream of the neck. There is no sign of any weak shock or a boundary as was shown in Fig. 5e.

A feature of the near body flow field shown in Figs. 4 and 5f is the separation shock emanating from the shoulder of the sphere. It is of interest to note that the diameter of the circle where the separation and wake shocks intersect is approximately equal to the width of the boundary delineated in Fig. 5e and the apparent inviscid wake width shown in Fig. 4. When two shock waves interact, the shapes of the shocks are slightly modified, and a slipstream is formed at the point of intersection. A horizontal knife-edge schlieren photograph of the near wake is shown in Fig. 5g. The inviscid wake, the viscous wake, and neck shock waves are clearly delineated. From a study of this photograph and that shown in Fig. 4, it is reasonable to conclude that at low hypersonic speeds the apparent inviscid wake may originate from the interaction of the separation and wake shock waves.

Goldburg (Ref. 9) has shown that the local Mach number at the maximum diameter of a sphere is approximately constant and equal to 3 for $M_\infty > 5$. The separation shock wave angle is dependent on the local Mach number. Since this Mach number is essentially constant, it is reasonable to assume that the separation shock wave angle is also essentially constant. The bow and wake shock wave angles well removed from the sphere are directly dependent on the free-stream Mach number and decrease with increasing Mach number. The variations in the wake and separation shock angles suggest that the diameter of their circle of intersection will increase with increasing speed. Therefore, it would be reasonable to expect the apparent inviscid wake diameter to increase with an increase in speed. Figure 6 presents results of some inviscid wake diameter measurements. There is a well-defined increase in the inviscid wake diameter with speed. This lends some support to the suggestion that the inviscid wake most often identified in flow field photographs may, in fact, originate from a shock interaction rather than from gas that has been processed through the almost normal part of the shock. Values of the inviscid wake diameter obtained in other facilities (Refs. 2 and 4) are compared with the VKF data in Fig. 6. Allowing for differences in judgment as to where the edge of this wake occurs, there is a good measure of agreement between these three sets of data. It cannot be overlooked that this wake property may be affected by ambient pressure. Clay, Labitt, and Slattery (Ref. 4) show a decrease in ambient pressure ($5 \leq p_\infty \leq 100$ mm Hg) produces a small increase in diameter. The VKF data presented in Fig. 6 cover a small pressure range ($10 \leq p_\infty \leq 50$ mm Hg), and a consistent effect of pressure is not evident.

The existence of the inviscid wake at high speeds has resulted in difficulties in determining the exact nature of the inner wake flow. Since an inviscid wake has been shown to exist at low velocities, it is also

necessary to consider the effect this can have on the interpretation of low-speed sphere wake data with regard to inner wake transition measurements. A consideration of Figs. 7a, b, and c suggests that a similar problem may exist at low speeds. The wake shown in Fig. 7a has the characteristics of a laminar wake in that no obvious undulations or perturbations are evident. If it is assumed that this is a laminar wake, two inconsistencies are evident:

1. The diameter of this wake is approximately three body diameters close to the body and does not vary out to $x/D = 65$. It has generally been accepted that laminar wakes grow slowly (cf., Ref. 4). For the inner, viscous laminar wake to grow to a diameter of three body diameters at $x/D = 5$ is not compatible with this assumption. Such a diameter is in fact compatible with the inviscid wake (or slipstream) generated by the separation- and wake-shock wave interaction (cf., Ref. 6).
2. A review of Slattery and Clay's data (Ref. 3) for 0.5-in. -diam spheres suggests that for the conditions under discussion transition should have occurred at $x/D = 20$.

As noted above, the wake in Fig. 7a appears to be laminar to $x/D = 65$. In comparing the present data with those contained in Ref. 3, it must be remembered that, whereas the present results were obtained with saboted spheres, those contained in Ref. 3 were obtained with unsaboted spheres. Birkhoff, et al. (Ref. 5) have also drawn attention to the effect of model surface condition at launch. They conclude it is reasonable to assume the unsaboted models have a rougher surface finish than the saboted models, and hence transition may occur sooner.

The observations made with regard to Fig. 7a also pertain to Fig. 7b. Figure 7c illustrates another problem related to the identification of low-speed transition onset. In this photograph there is clear evidence of turbulence. The degree of turbulence appears to increase as x/D increases from 53 to 113. The diameter of this wake is approximately four body diameters, which is the diameter of the inviscid wake for this speed (cf., Fig. 6). The average diameter of the turbulent wake (Ref. 3) in this region in the wake is approximately three body diameters. Therefore, it would be reasonable to expect portions of the turbulent wake to burst intermittently through the inviscid wake edge, as is in fact shown in Fig. 7c. Birkhoff, et al. (Ref. 5) present a similar photograph to that shown in Fig. 7c. Their assessment of the photograph is, "Turbulent segments of viscous sphere wakes may be separated by much longer laminar segments, so that the wake displays intermittent turbulence (This is "turbulence in bursts," as described in other situations by Howard Emmons. . .) over much of its length."

Although this very well may occur, such an interpretation does not explain the events portrayed in Fig. 7c or in other cases when consideration is given to the coexistence of inviscid, outer, and turbulent inner wakes of near-equal diameters. Then, the intermittent "bursts" may simply represent incipient breakthrough.

The high-speed case which has received considerable attention because of its greater interest in relation to reentry body studies will now be considered. At low speeds the weak shock waves originating at the turbulent wake edge do not appear to penetrate the inviscid wake boundary (Fig. 5e). At high speeds (Fig. 8a) the sphere wake flow field is characterized by a large number of weak shock waves apparently emanating from the turbulent wake. A study of the upper photograph in Fig. 8a reveals a turbulent inner wake close to the body and a clearly defined shock interaction boundary. The lower photographs in Figs. 8a and b appear to confirm that the weak shocks originate at the turbulent wake edge. On the basis of this evidence it is reasonable to conclude that the existence of these waves indicates the presence of a turbulent inner wake. At low ambient pressures where the sensitivity limit of the schlieren system is approached, these weak shocks may no longer be visible. Therefore, for these flight conditions (i. e., high speed and low ambient pressure) the fact that these shocks are not present does not necessarily mean that the inner wake is laminar.

In Ref. 6 it has been suggested that the occurrence of these weak waves in the outer wake in the absence of definite indications of turbulence outside the inviscid wake means that the inner wake is turbulent. Therefore, the first occurrence of such waves is a reasonable limit on the most rearward location of transition in the inner wake. The occurrence of these waves is taken (Wilson, Ref. 2) to indicate the onset of incipient breakthrough, i. e., the diameter of the turbulent inner wake is approximately equal to the inviscid wake diameter.

Clay, Labitt, and Slattery (Ref. 4) designate the occurrence of visible turbulence of the type shown in the lower photograph (Fig. 8a) as the onset of transition. This does not appear to be an accurate assessment of the state of the inner wake.

3.3 BREAKTHROUGH

In this discussion breakthrough is defined as occurring at that axial station in the wake where the inviscid wake first is totally engulfed by the turbulent inner wake. It has been so described in Ref. 2, "The general character of turbulent breakthrough at all Reynolds numbers

above 10^5 is the same for all spherical bodies, with the breakthrough occurring always about 150 body diameters behind the body."

Some of the practical problems of identifying breakthrough will now be discussed. The upper photograph in Fig. 8b indicates that the inviscid wake has been completely engulfed by the turbulent inner wake at an axial distance of approximately 190 body diameters, in reasonable agreement with the above statement. Figures 9a and b present additional far wake flow field photographs. In Fig. 9a breakthrough appears to occur at $x/D = 330$, whereas it occurs at an $x/D = 230$ for the sphere shown in Fig. 9b. It is important to realize that for these two cases, the Reynolds number and velocity were very nearly equal. These values of distance to breakthrough, x/D , do not agree with each other or with Wilson's suggested value of 150. These differences suggest that in the high Reynolds number flow regime breakthrough may not be a well-defined phenomenon because it will be clear to the reader that individual judgment plays a powerful role in deciding where breakthrough occurs in any of these photographs.

As the intermediate Reynolds number regime (i. e., $Re_m = 10^5$) is approached, a consideration of the lower photograph in Fig. 8a indicates that breakthrough becomes more difficult to define. For these conditions, portions of the inviscid wake are totally engulfed by the turbulent inner wake. Such regions are separated by regions of wholly smooth flow. At what point then does it become possible to say breakthrough has occurred?

Figures 10a, b, and c present a sequence of vertical (with the direction of flight) knife-edge photographs of sphere wakes at Reynolds numbers comparable to that given in the lower photograph of Fig. 8a. Figure 10b presents a photograph at the same axial location, velocity, and Reynolds number as in this figure. The following features of the flow field are of interest:

1. Weak shock waves originating at the turbulent wake edge, and
2. Fully turbulent inner wake.

Perhaps the most striking feature is the absence of the inviscid wake. Figure 10a also shows a complete absence of an inviscid wake closer to the body. (The lower half of this photograph has less sensitivity than the upper half. This can be seen from the total absence of the weak shock waves in this half of the photograph. It has been concluded that this loss in sensitivity has resulted from errors in the schlieren optical setup.)

The presence of weak shock waves in the outer flow field at $x/D = 500$ indicates that the wake edge is traveling at supersonic speeds with respect to the nearby flow. Figure 10d demonstrates the capability of the framing camera and continuous light source to produce photographs of a turbulent far wake. Close to the body (i.e., $x/D \leq 1000$), the exposure duration of the film is too long for useful photographs of the model and wake to be made.

A schlieren system with a knife edge normal to the direction of flight is insensitive to radial density gradients. Therefore, such a system is insensitive to laminar and inviscid wakes, which exhibit only small axial gradients, but is highly sensitive to turbulent wake flow, characterized by gradients in all directions. The above-discussed comparison of Figs. 8a and 10a and b clearly demonstrates these properties of schlieren systems when used with "vertical" and "horizontal" knife edges.

It follows that, whereas with a "horizontal" knife edge the inner, viscous wake appears largely obscured by large gradients of the larger diameter, inviscid wake, with a "vertical" knife edge the schlieren effect of the inviscid wake is eliminated, and a turbulent wake, even when shrouded by a strong inviscid wake, is well defined in the schlieren picture.

Clearly, then, the use of schlieren system in the two modes is required for precise determination of (1) onset of wake turbulence and (2) location of "breakthrough," or region in which the turbulent wake engulfs the inviscid wake.

It is of interest to consider the respective diameters of the turbulent inner wake and the inviscid wake. Measurements have been made of the turbulent wake diameter. These diameters have been derived by tracing the boundary of the turbulent wake with a planimeter and averaging the width over a distance of at least 10 body diameters. A comparison of this diameter and inviscid wake diameter for approximately the same flight conditions is made in Fig. 11. For these flight conditions the turbulent wake will always have burst through the inviscid wake for $x/D \leq 400$. Because the average wake width is being considered, it is obvious that the turbulent edge of the inner wake will be visible closer to the body than $x/D \leq 400$.

3.4 LOW REYNOLDS NUMBER WAKE

Until now we have considered sphere wakes at Reynolds numbers of 1.25×10^5 or greater. A characteristic of such wakes is that turbulence

must have occurred close to the body, (cf., Figs. 8 through 10) where, in this context, close to the body implies $x/D < 400$. Figure 12 presents a sequence of wake photographs obtained for $Re_\infty = 8.1 \times 10^4$. These wake photographs illustrate very clearly the radical change in the character of the wake as the Reynolds number is reduced from $Re_\infty = 1.25 \times 10^5$ (Figs. 10a and c) to $Re_\infty = 8.1 \times 10^4$. The first detectable instability in the wake occurs at $x/D = 3000$. At this axial station, Fig. 11 indicates that a turbulent inner wake would have a diameter of approximately 13 body diameters. Such a diameter would be approximately twice that of the inviscid wake observed for $x/D = 3000$. This suggests that turbulence of the type discussed earlier for $Re_\infty \geq 1.25 \times 10^5$ does not occur close to the body for $Re_\infty = 8.1 \times 10^4$.

Wilson (Ref. 2) has also observed this same radical change toward increased stability in the wake flow field for $Re_\infty \leq 10^5$. This very gradual transition to turbulence in the laminar wake of a high-speed cone is illustrated in Fig. 13. Both wakes are characterized by the existence of smoothly undulating filaments. It has been shown elsewhere (e. g., Ref. 1) that cone wakes of this type (Fig. 13) do become fully turbulent. Initially the sphere wake consists of smooth undulating filaments. In time these filaments roughen, but still retain the gross undulations. Finally, the gross undulations merge with one another, resulting in a fully turbulent wake. These framing camera sequences have, as suggested earlier, resulted in some degradation in definition. Figures 14a, b, c, and d present a series of single-spark schlieren photographs obtained for $Re_\infty = 5^4$. Several of the photographs in this series bear a strong resemblance to the laminar flow breakup of the cone wake in Fig. 13.

Fay and Goldburg (Ref. 15) have made extensive studies of the structure of the sphere wake at low Reynolds numbers. The technique used was to study the visible radiation patterns of bluff body wakes, where the radiation was enhanced by the presence of small quantities of ablating material. As a result of these studies, Fay and Goldburg suggest the presence of hypersonic vortex shedding, which bears a strong resemblance to subsonic vortex patterns obtained for incompressible wakes by Margarvey and Bishop (Refs. 16 through 18). These incompressible wake patterns have been obtained by studying the motion of a droplet of carbon tetrachloride, with a dye, falling through water. Examples of wake patterns obtained in this manner at AEDC are shown in Fig. 15. Margarvey and Bishop (Ref. 18) have identified six distinct wake patterns:

1. Single thread,
2. Double thread,
3. Double thread with waves,

4. Procession of vortex loops,
5. Double row of vortex rings, and
6. Asymmetrical wake.

Figure 15 presents examples of types 3 and 4. Fay and Goldburg (Ref. 15) suggest the vortex loop wake shown in Fig. 15 is the three-dimensional counterpart of the von Kármán vortex sheet behind a cylinder. Figures 14a and b contain photographs which bear a resemblance to the incompressible wake patterns shown in Fig. 15. This similarity appears to substantiate Fay and Goldburg's postulation of hypersonic vortex shedding.

It has been observed in Fig. 12 that the smooth undulating wake breaks up into a rough undulating wake. This process has also been suggested by Fay and Goldburg. This particular wake characteristic may shed some light on wake phenomena observed at higher Reynolds numbers. When the orthogonal shadowgrams in Fig. 4 were discussed earlier, it was pointed out that there were some large-scale undulations superposed on the turbulent wake. Such undulations at these high Reynolds numbers will merge more quickly and seem less pronounced than for the cases shown in Figs. 12 and 13. However, if such undulations exist at low speeds and Reynolds numbers, it is possible that a similar but less clear behavior could be confused with "intermittent turbulence" in some cases.

Fay and Goldburg (Ref. 15) have assumed that the products of ablation necessary for their visualization technique do not affect the fluid dynamic nature of the flow. At low Reynolds numbers (i. e., $Re_{\infty} \leq 10^5$), Wilson's (Ref. 2) measurements of the distance to the first signs of turbulence have been shown to be unaffected by the presence of the products of ablation. It has been shown in Fig. 12 that the first instabilities in wake flow for a copper sphere ($Re_{\infty} = 8.1 \times 10^4$) occur at $x/D = 3000$. This value is in good agreement with Wilson's (Ref. 2) measurements at the same Reynolds number. Figures 16a and b show wake photographs of copper, nylon, and aluminum spheres at similar flight speeds to that represented in Fig. 12. At the same axial station in the wake, the ablating nylon and aluminum models show evidence of strong wake turbulence at $x/D \approx 1000$. This would seem to be too large a difference to be explained simply in terms of data scatter. The problem is further emphasized by the fact that at $Re_{\infty} \approx 3.3 \times 10^4$ an ablating nylon sphere indicates turbulence at $x/D = 500$ in Fig. 16b. These results indicate that there is, under some conditions, a marked effect of ablation on turbulence onset.

Figures 17a through f present sequences of wake flow field patterns obtained with the framing camera for $Re_{\infty} = 5 \times 10^4$. Variations in model diameter, ambient pressure, and velocity have been such that the Reynolds number was constant. It is assumed, on the basis of data presented in Ref. 8, for these flight conditions the copper spheres did not ablate. A detailed study of these sequences reveals a similarity between the observed patterns and those shown for the incompressible wake (Fig. 15). There is a variation in the location of the first signs of turbulence. However, such a variation may reflect the basic unpredictability of events such as this.

SECTION IV CONCLUSIONS

As a result of the present studies the definition of the inviscid wake must be questioned. Data are presented which indicate the possibility of a slipstream, originating at the intersection of the separation and wake shocks, being mistaken for the inviscid wake as it is defined in Ref. 1. (See Section I of this report.) Photographs clearly showing an apparent inviscid wake at supersonic and low hypersonic speeds are in disagreement with the concept of the inviscid wake occurring only at or near reentry speeds. It is readily agreed that at high speeds the apparent inviscid wake has shielded details of the inner wake, when observed with a horizontal knife-edge schlieren system. The demonstrated existence of such a wake at low speeds indicates probable misinterpretation of low-speed data (cf., Ref. 5). In such cases the apparent inviscid (outer) wake has been mistakenly called a laminar inner wake.

Comparison of wake visualization with schlieren systems having vertical and horizontal knife edges demonstrates that for adequate definition of turbulent wakes of spheres (or blunt bodies in general), both modes of schlieren visualization are necessary.

Examination of wake observations suggests that for spheres, the apparent "inviscid" wake boundary may originate from interaction of wake shock and separation shock, rather than correspond to the "edge" of the gas volume which has been processed through the "almost normal" portion of the bow shock. Should this interpretation be correct, the significance of "breakthrough" as related to radar returns from wakes of spheres may be in doubt, since, in this case, the inviscid wake would not be sufficiently ionized to shield the inner, turbulent wake.

The many wake photographs shown for $Re_{\infty} \leq 10^5$ are indicative of a large-scale vortex shedding phenomenon. Striking similarities between the schlieren-observed trails of hypersonic spheres and the low-speed incompressible wakes of bluff bodies have been observed. For $Re_{\infty} \leq 10^5$ the onset of flow instabilities in the sphere wake undergoes a very rapid rearward shift.

REFERENCES

1. Wilson, L. N. "Body Shape Effects on Axisymmetric Wakes." General Motors Corporation, TR-64-02K, October 1964.
2. Wilson, L. N. "The Far Wake Behavior of Hypersonic Spheres." General Motors Corporation, TR-66-19, June 1966.
3. Slattery, R. E. and Clay, W. G. "The Turbulent Wake of Hypersonic Bodies." American Rocket Society 17th Annual Meeting and Space Flight Exposition, No. 2673-62, November 13 through 18, 1962.
4. Clay, W. G., Labitt, M., and Slattery, R. E. "Measured Transition from Laminar to Turbulent Flow and Subsequent Growth of Turbulent Wakes." AIAA Journal, Vol. 3, No. 5, May 1965, pp. 837-846.
5. Birkhoff, G., Eckerman, J., and McKay, W. "Transition and Turbulence in Hypersonic Wakes." The Physics of Fluids, Vol. 9, No. 3, March 1966, pp. 446-452.
6. Bailey, A. B. "Turbulent Wake and Shock Shape of Hypervelocity Spheres." AEDC-TR-66-32 (AD484821), July 1966.
7. Demetriades, Anthony and Gold, Harris. "Transition to Turbulence in the Hypersonic Wake of Blunt-Bluff Bodies." American Rocket Society, September 1962, pp. 1420-1421.
8. Hendrix, R. E. and Bailey, A. B. "Radar Study of Sphere Wakes." AEDC-TR-66-182 (AD802526), November 1966.
9. Goldberg, Arnold. "A Summary Analysis of Laboratory Hypersonic Wake Fluid Mechanics Transition Experiments." AIAA 5th Aerospace Sciences Meeting, Paper No. 67-33.
10. Primich, R. I., Robillard, P. E., Eschenroeder, A. Q., Wilson, L., and Zivanovic, S. "Radar Scattering from Wakes." General Motors Corporation TR-65-01E, March 1965.

11. Zivanovic, S., Robillard, P. E., and Primich, R. J. "Radar Investigation of the Wakes of Blunt and Slender Hypersonic Velocity Projectiles in the Ballistic Range." AC Electronics - Defense Research Laboratories, General Motors Corporation, TR-67-01C, 1967.
12. Reis, V. H. "Chemiluminescent Radiation in the Far Wakes of Hypersonic Spheres." AIAA Journal, Vol. 5, No. 11, 1967, pp. 1928-1933.
13. Clemens, P. L. "The von Kármán Gas Dynamics Facility 1000-ft Hypervelocity Range - Description, Capabilities and Early Test Results." AEDC-TR-66-197 (AD801906), November 1966.
14. Lees, L. "Hypersonic Wakes and Trails." AIAA Journal, Vol. 2, No. 3, 1964, pp. 417-420.
15. Fay, J. A. and Goldburg, A. "Unsteady Hypersonic Wake behind Blunt Bodies." AIAA Journal, Vol. 1, No. 10, 1963, pp. 2264-2272.
16. Margarvey, R. H. and Bishop, R. L. "The Wake of a Moving Drop." Nature, No. 188, 1960, pp. 735-736.
17. Margarvey, R. H. and Bishop, R. L. "Wakes in Liquid-Liquid Systems." Physics of Fluids, Vol. 4, 1961, pp. 800-805.
18. Margarvey, R. H. and Bishop, R. L. "Transition Ranges for Three-Dimensional Wakes." Canadian Journal of Physics, Vol. 39, 1961, pp. 14218-14222.

**APPENDIX
ILLUSTRATIONS**

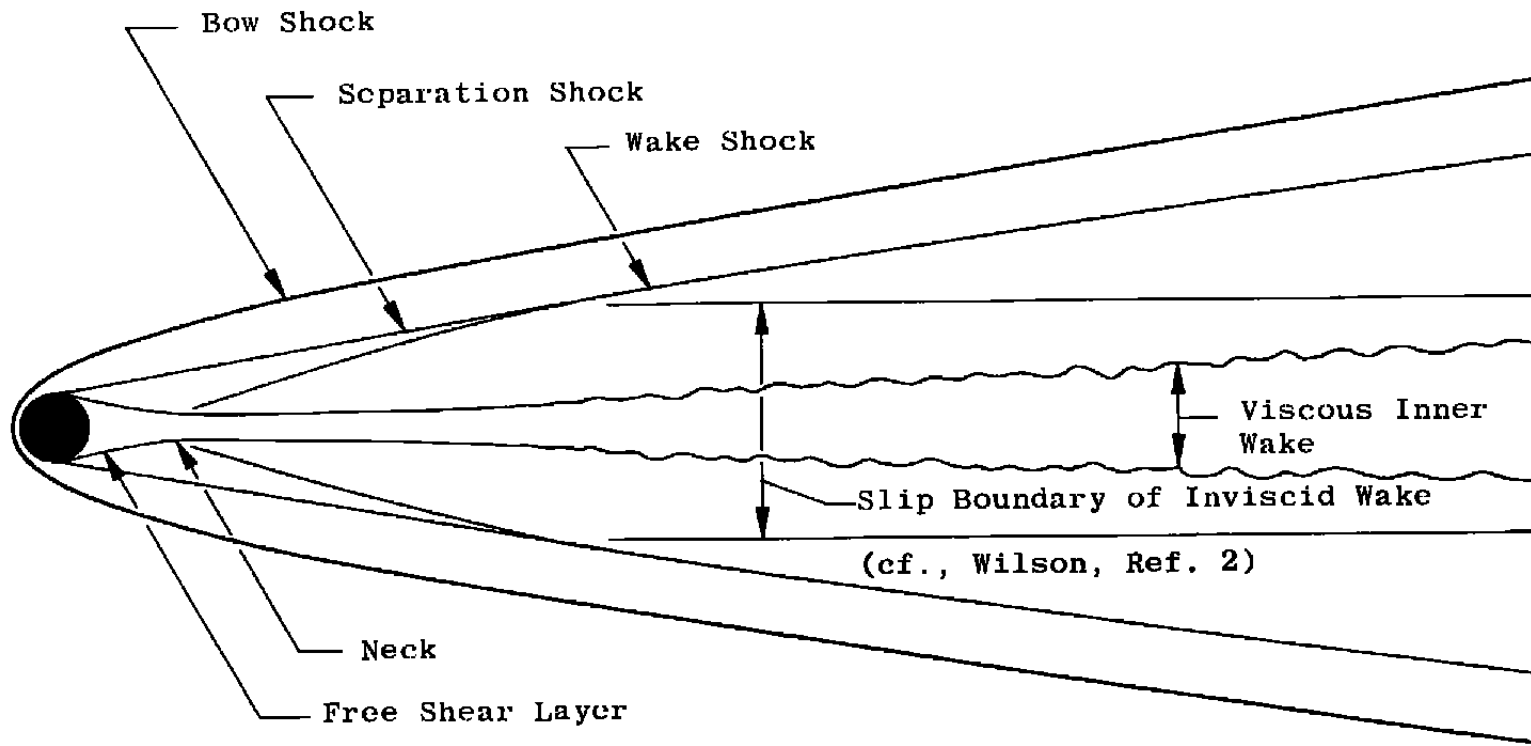


Fig. 1 Flow Field of a Hypersonic Sphere

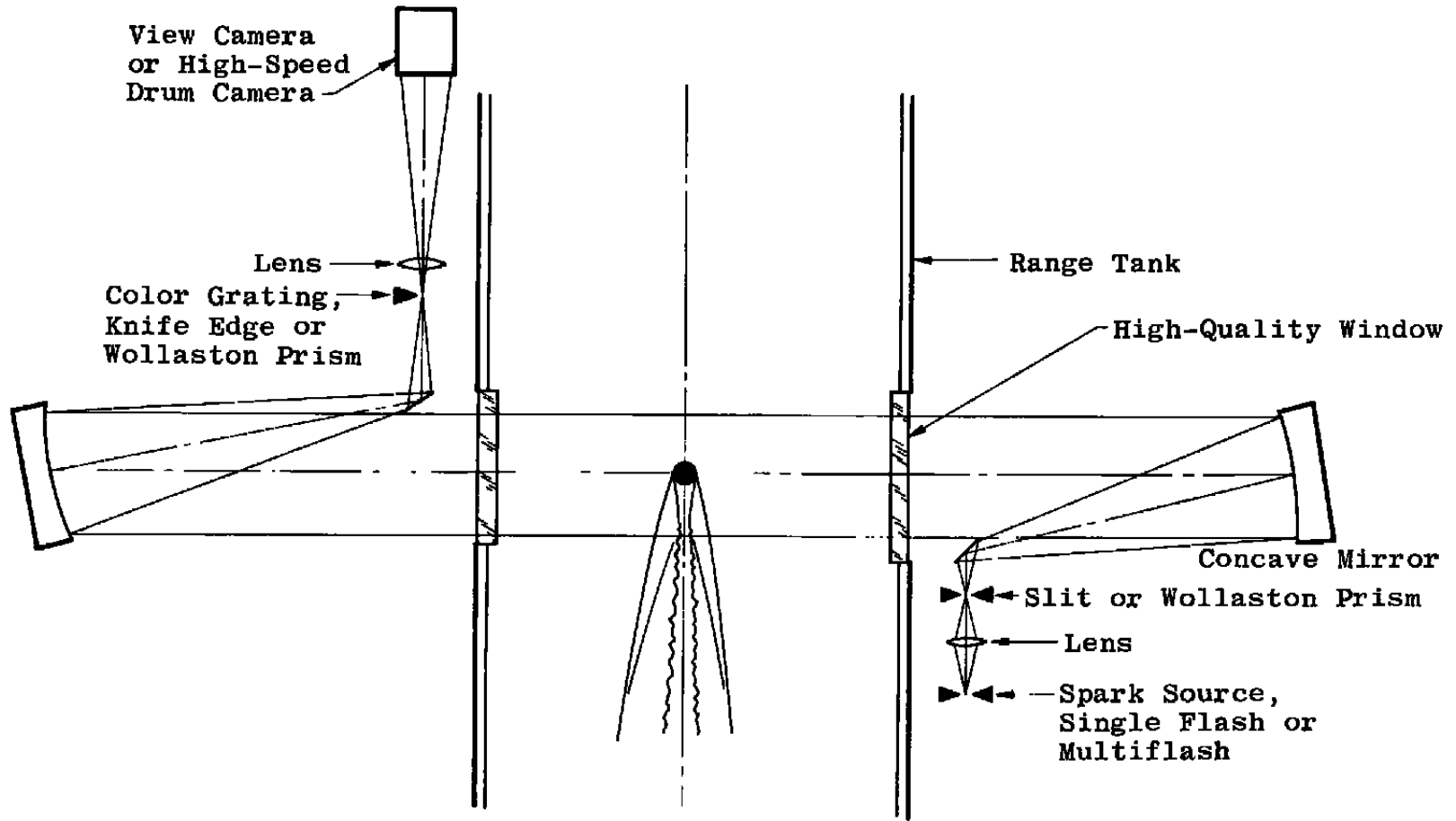


Fig. 2 Single-Pass Schlieren System

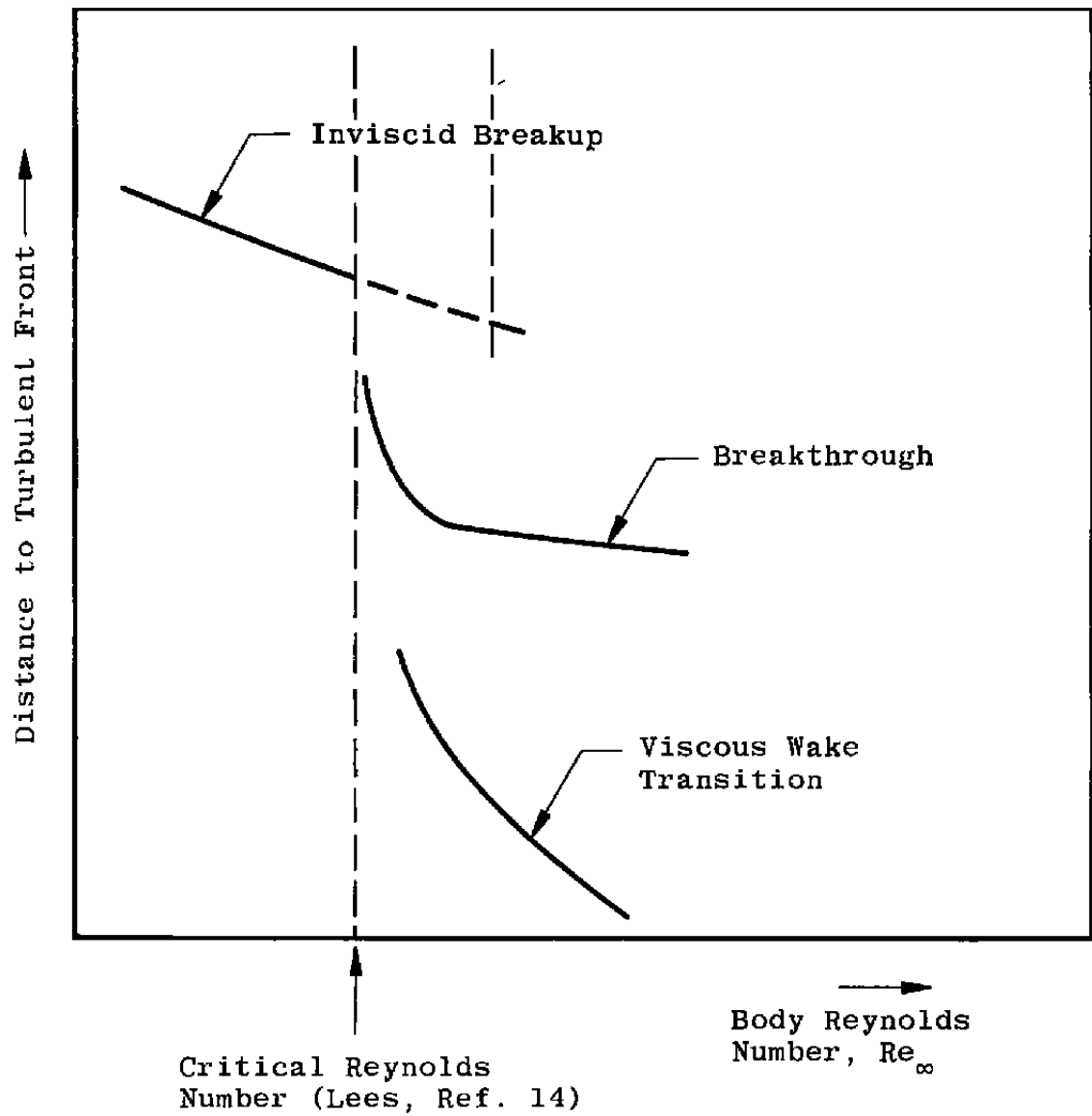


Fig. 3 Expected Location of Inviscid Breakup and Turbulence Breakthrough
(Attributable to Wilson, Ref. 2)

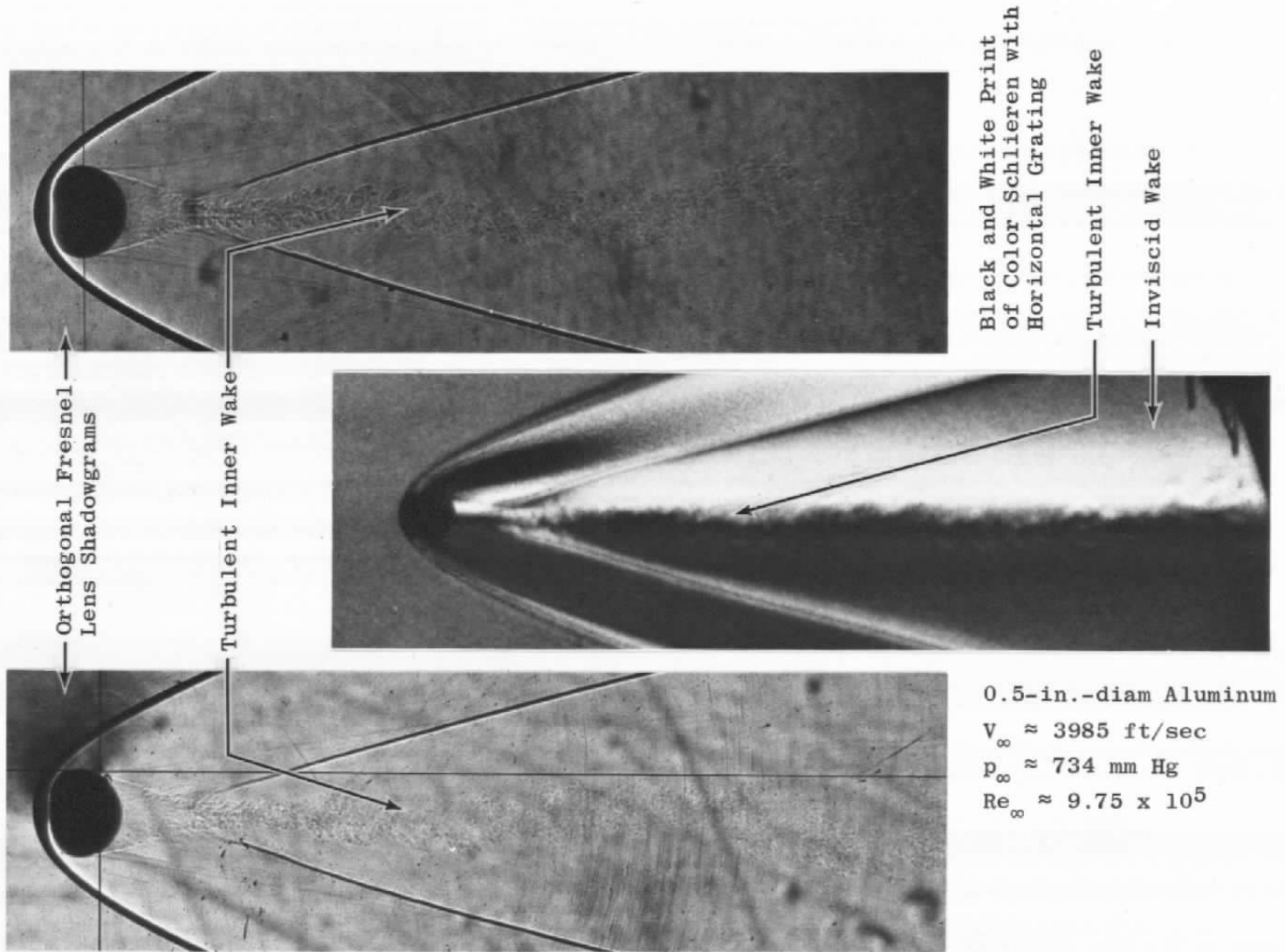
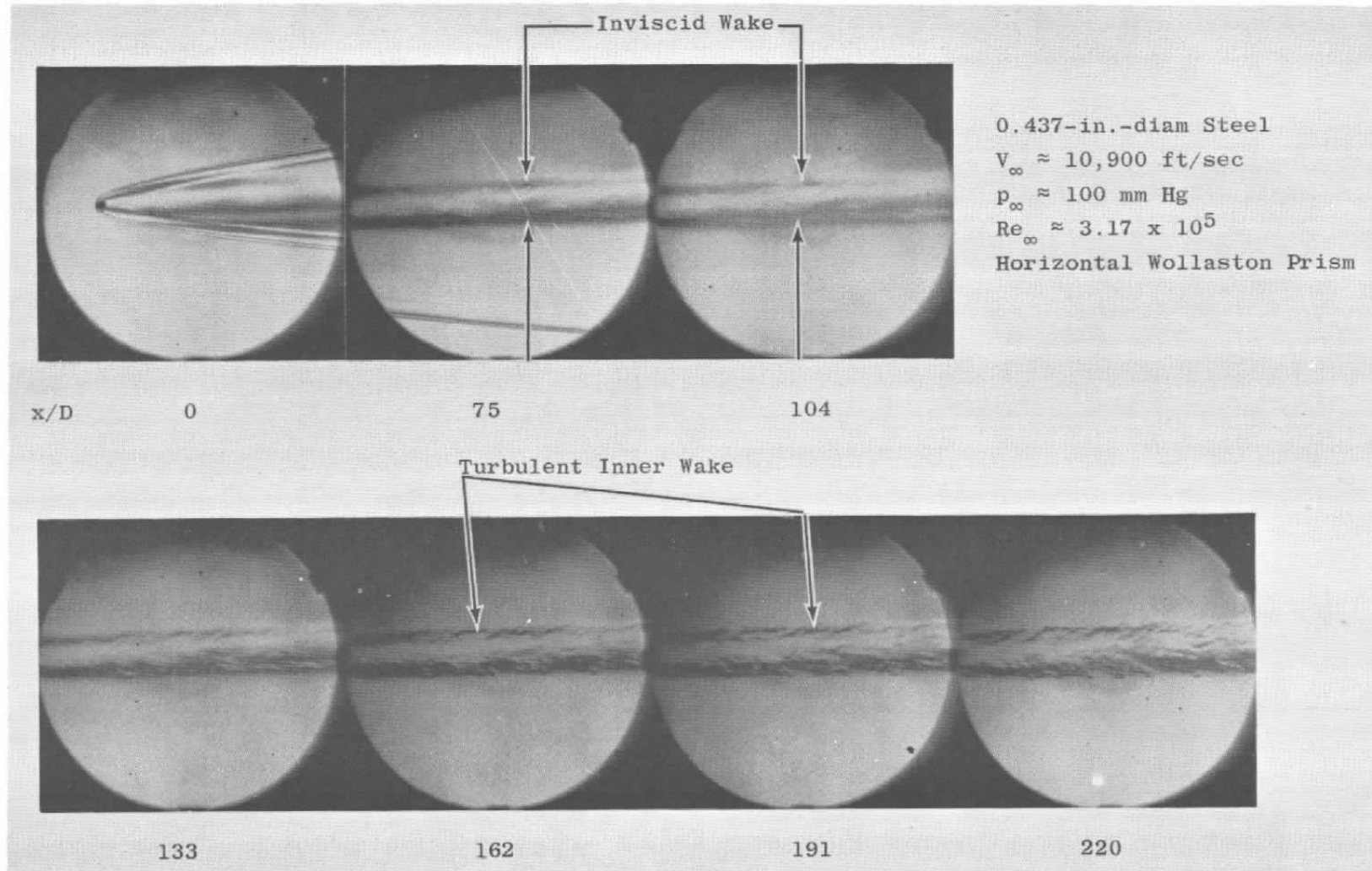
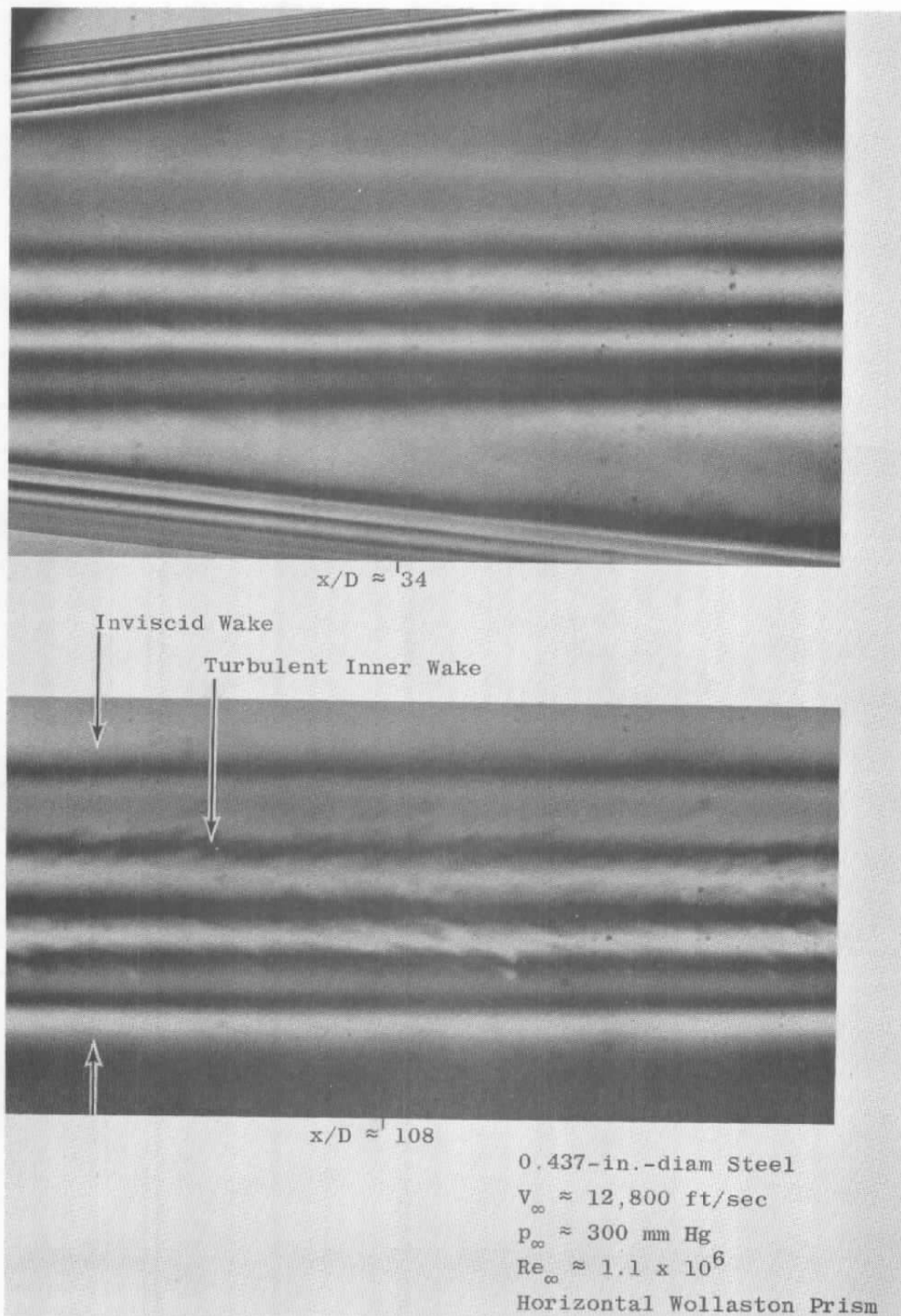


Fig. 4 Flow Field of a Supersonic Sphere



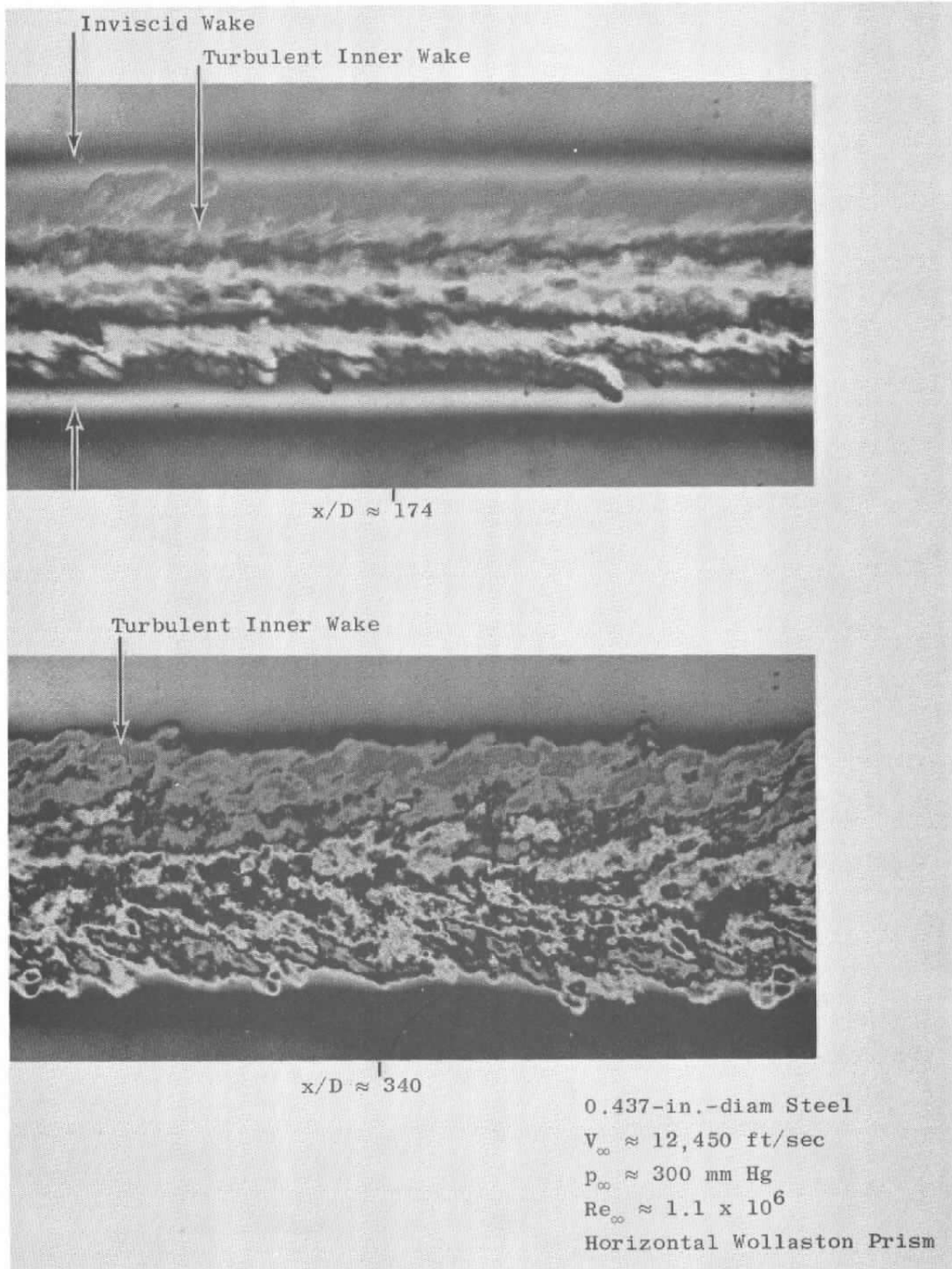
a. $V_{\infty} \approx 10,900$ ft/sec, $p_{\infty} \approx 100$ mm Hg, and $Re_{\infty} \approx 3.17 \times 10^5$

Fig. 5 Wake Flow Field of a Sphere at Low Hypersonic Speeds



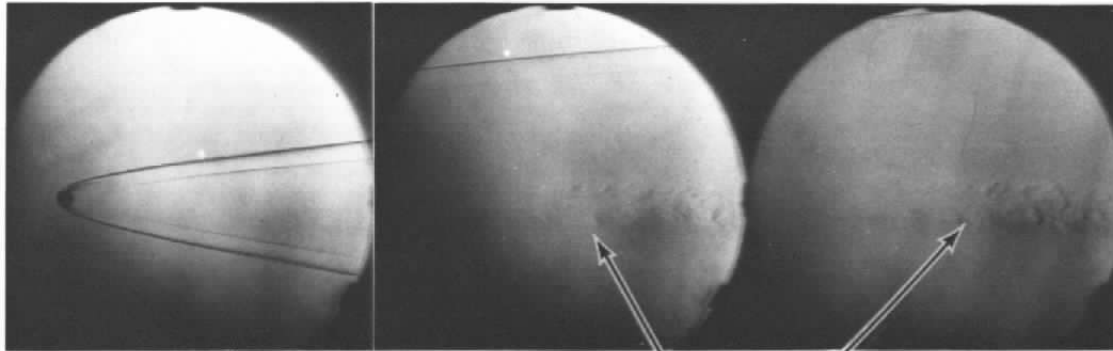
b. $V_\infty \approx 12,800$ ft/sec, $p_\infty \approx 300$ mm Hg, and $Re_\infty \approx 1.1 \times 10^6$

Fig. 5 Continued



c. $V_\infty = 12,450$ ft/sec, $p_\infty = 300$ mm Hg, and $Re_\infty = 1.1 \times 10^6$

Fig. 5 Continued



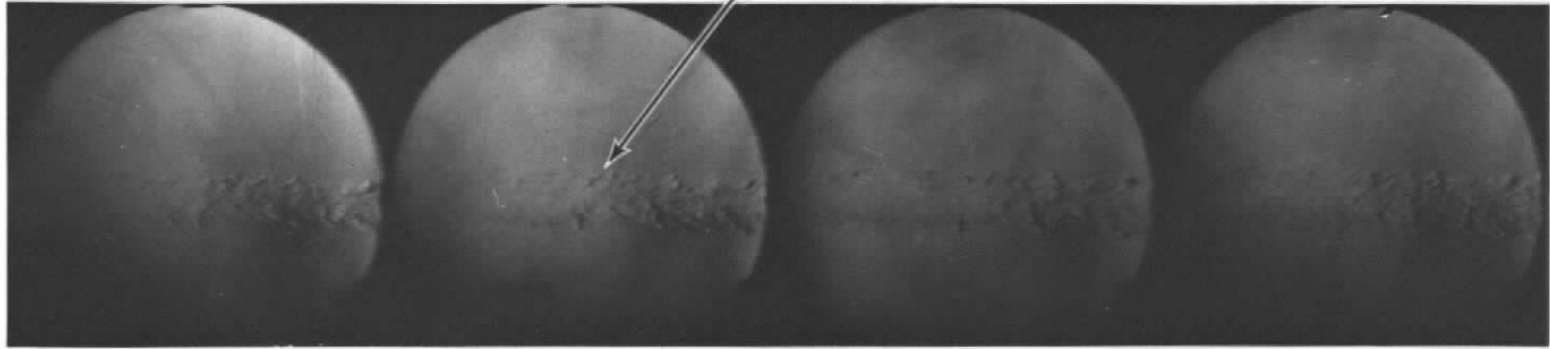
0.437-in.-diam Steel
 $V_\infty \approx 10,600$ ft/sec
 $p_\infty \approx 100$ mm Hg
 $Re_\infty \approx 3.08 \times 10^5$
 Vertical Wollaston Prism

0

68

95

Turbulent Inner Wake



122

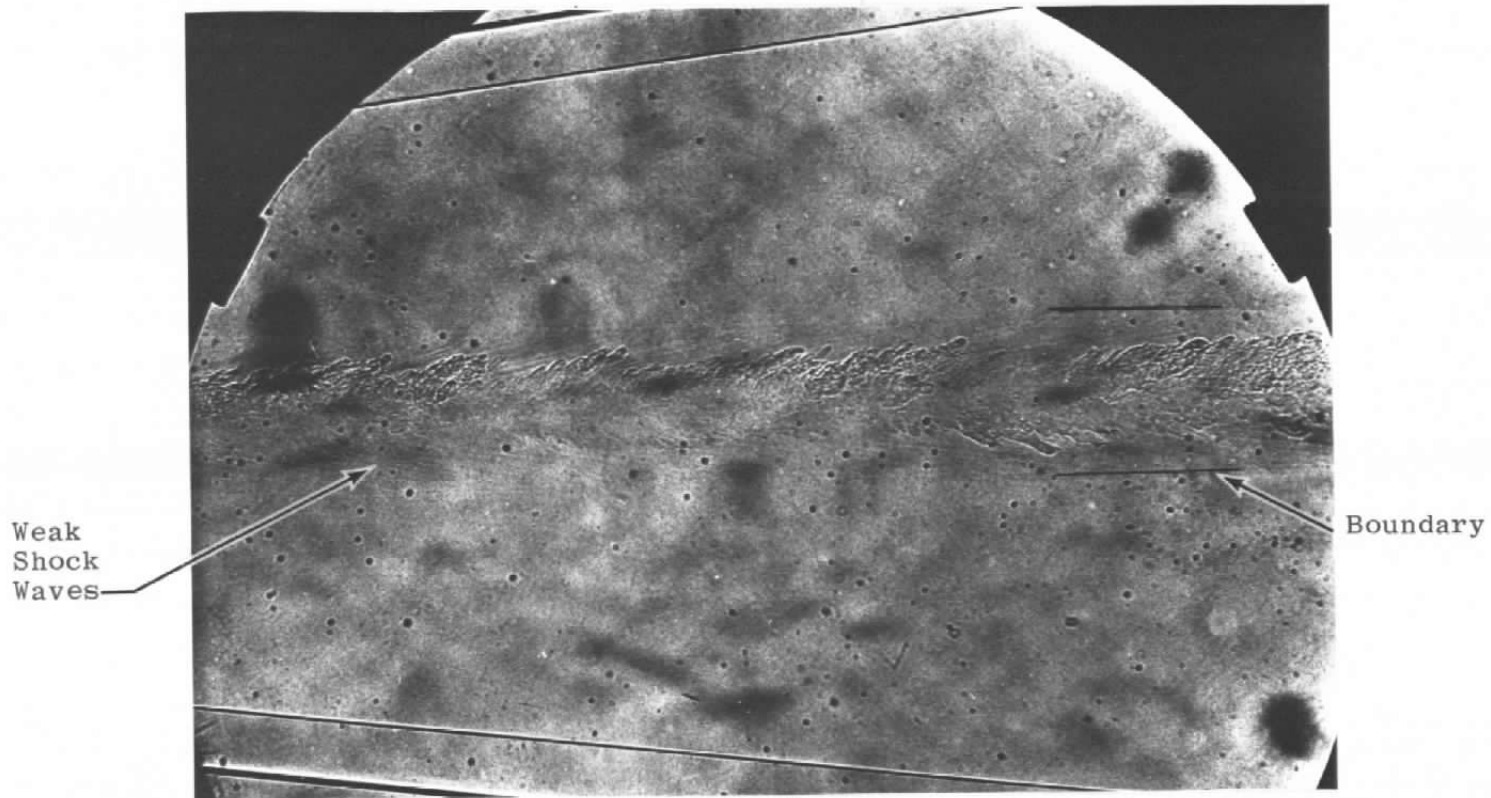
150

177

205

d. $V_\infty \approx 10,600$ ft/sec, $p_\infty \approx 100$ mm Hg, and $Re_\infty \approx 3.08 \times 10^5$

Fig. 5 Continued

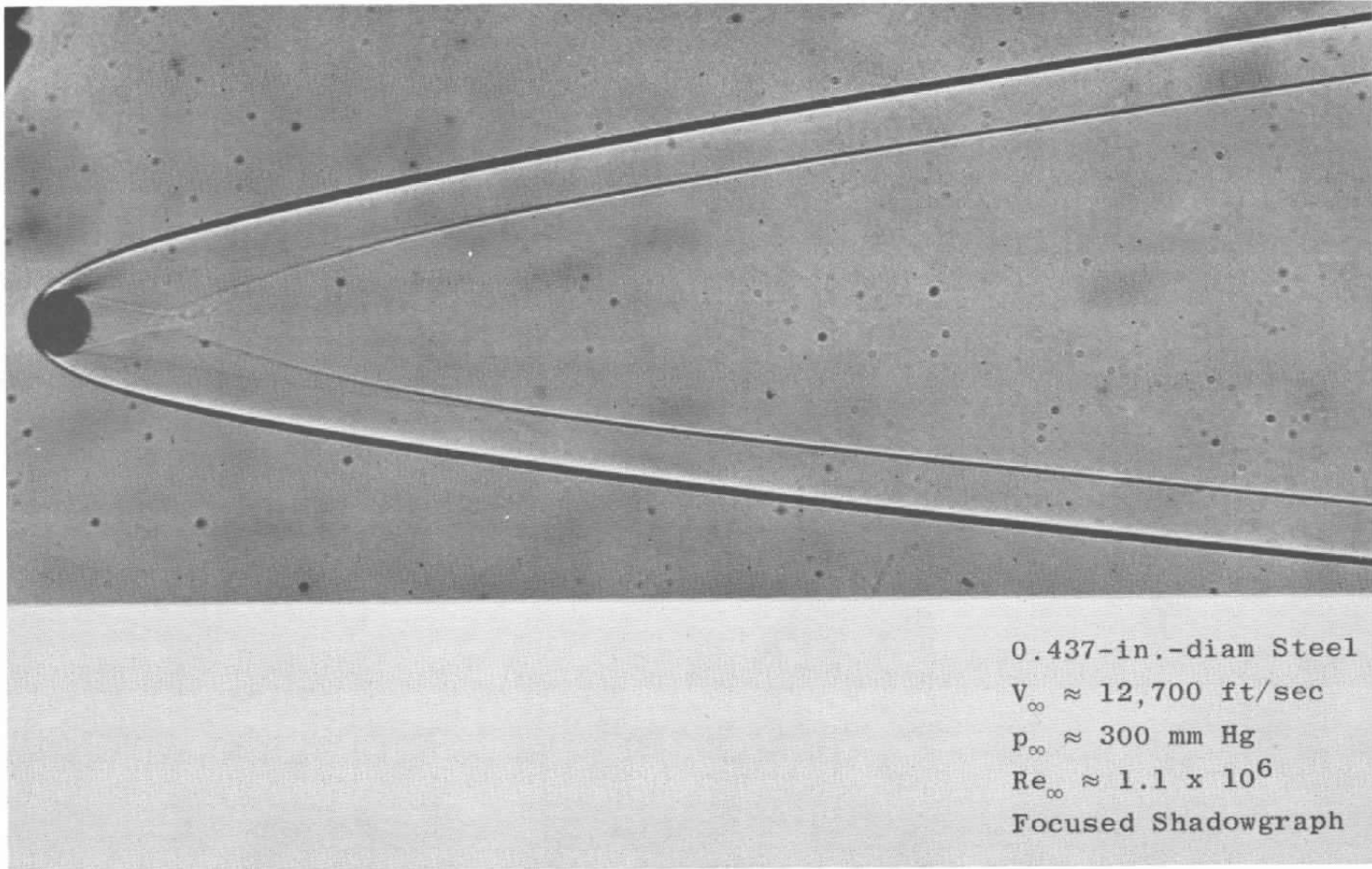


$x/D \approx 48$

0.437-in.-diam Steel
 $V_\infty \approx 9500$ ft/sec
 $p_\infty \approx 600$ mm Hg
 $Re_\infty \approx 1.65 \times 10^6$
 Focused Shadowgraph

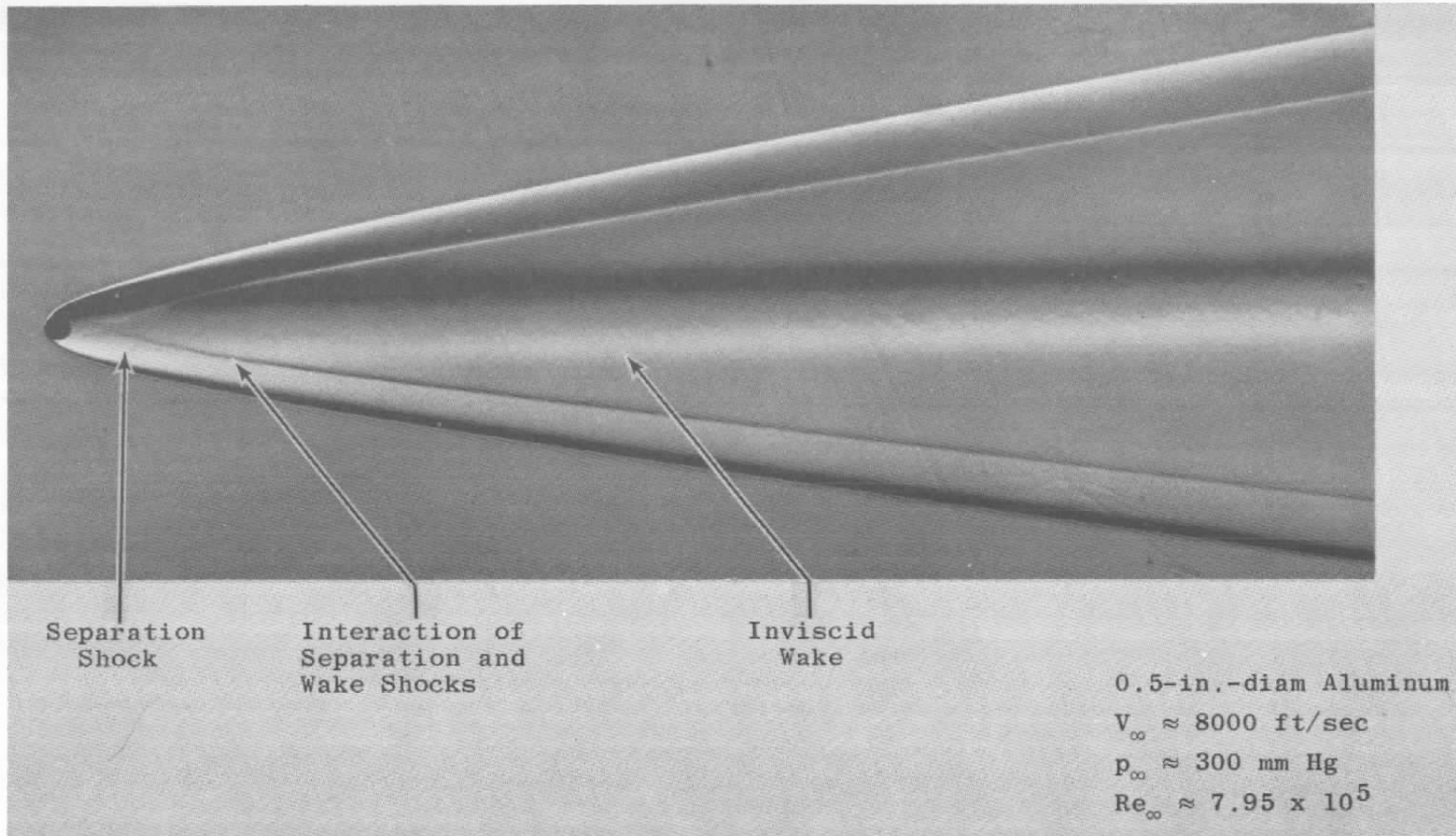
e. $V_\infty \approx 9500$ ft/sec, $p_\infty \approx 600$ mm Hg, and $Re_\infty \approx 1.65 \times 10^6$

Fig. 5 Continued



f. $V_\infty = 12,700$ ft/sec, $p_\infty = 300$ mm Hg, and $Re_\infty = 1.1 \times 10^6$

Fig. 5 Continued



g. $V_{\infty} \approx 8000$ ft/sec, $p_{\infty} \approx 300$ mm Hg, and $Re_{\infty} \approx 7.95 \times 10^5$

Fig. 5 Concluded

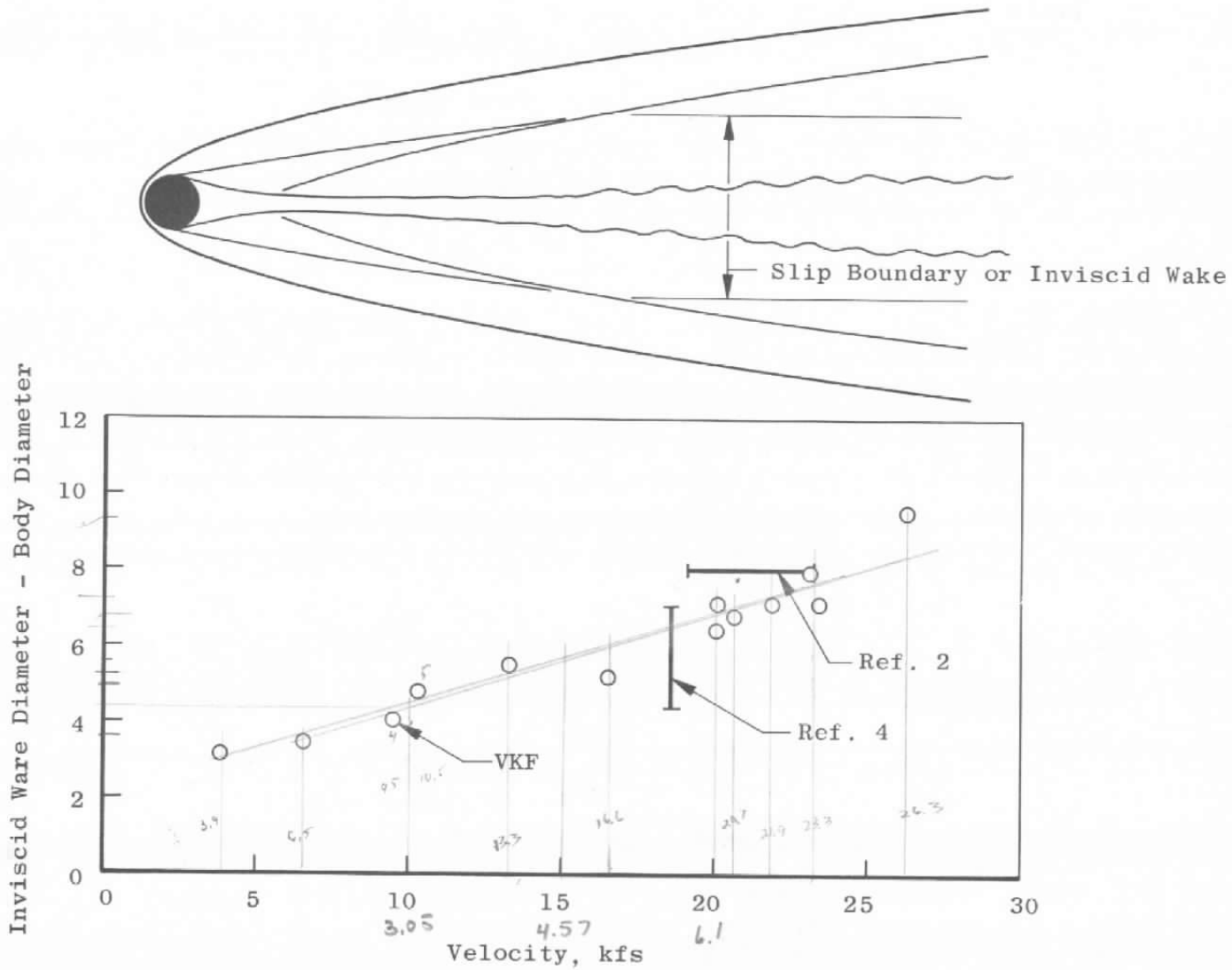
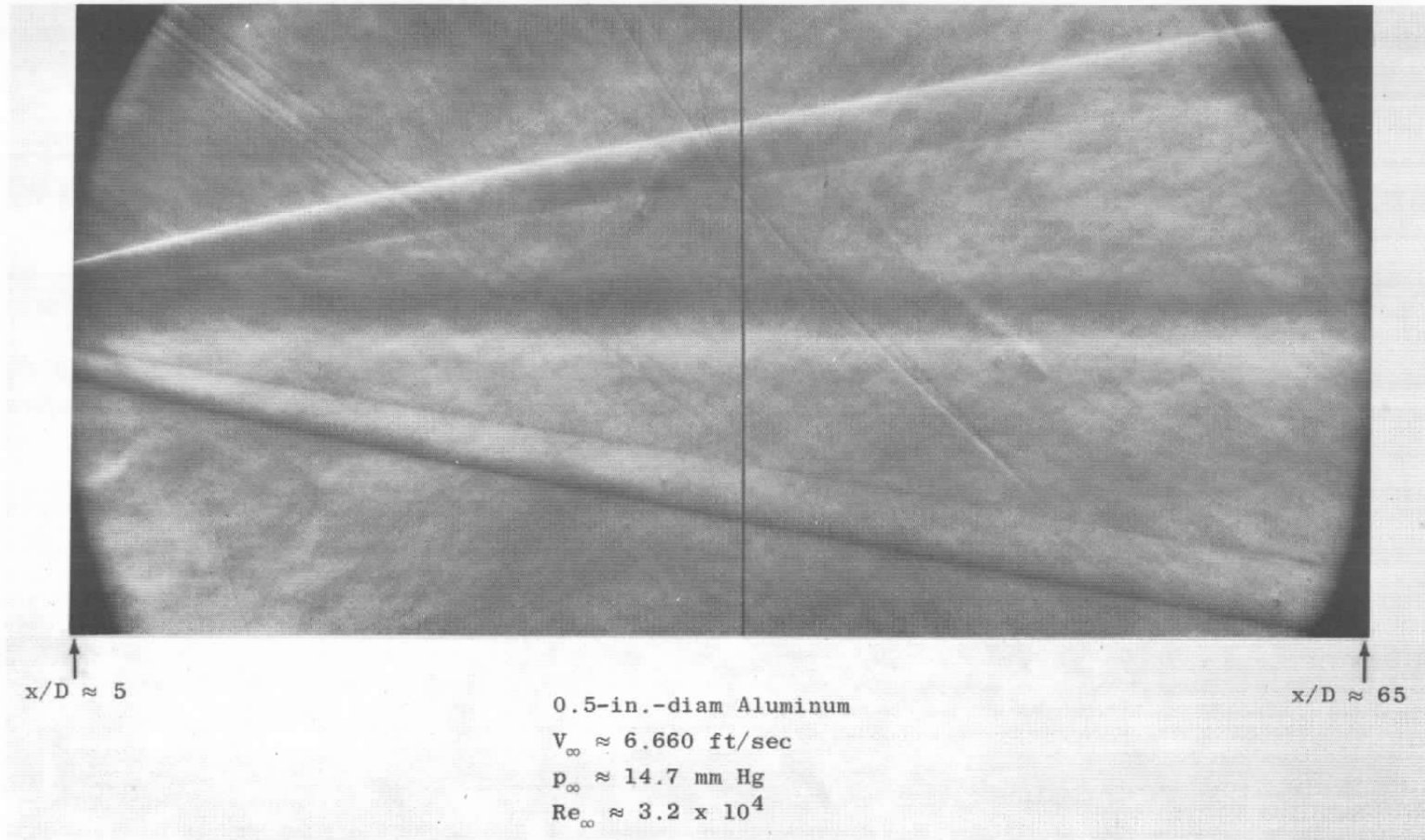
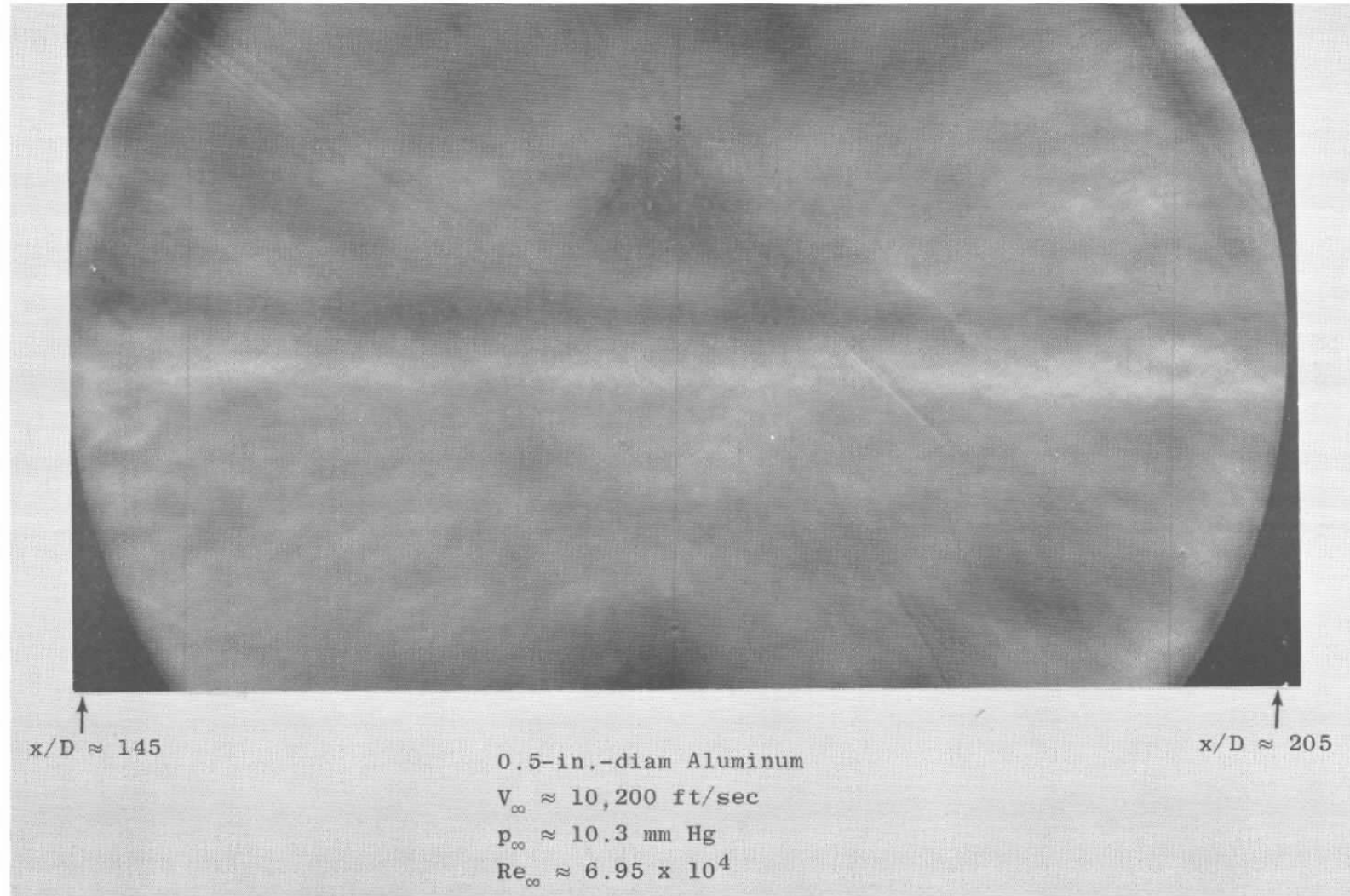


Fig. 6 Variation of Inviscid Wake Diameter with Velocity for Spheres



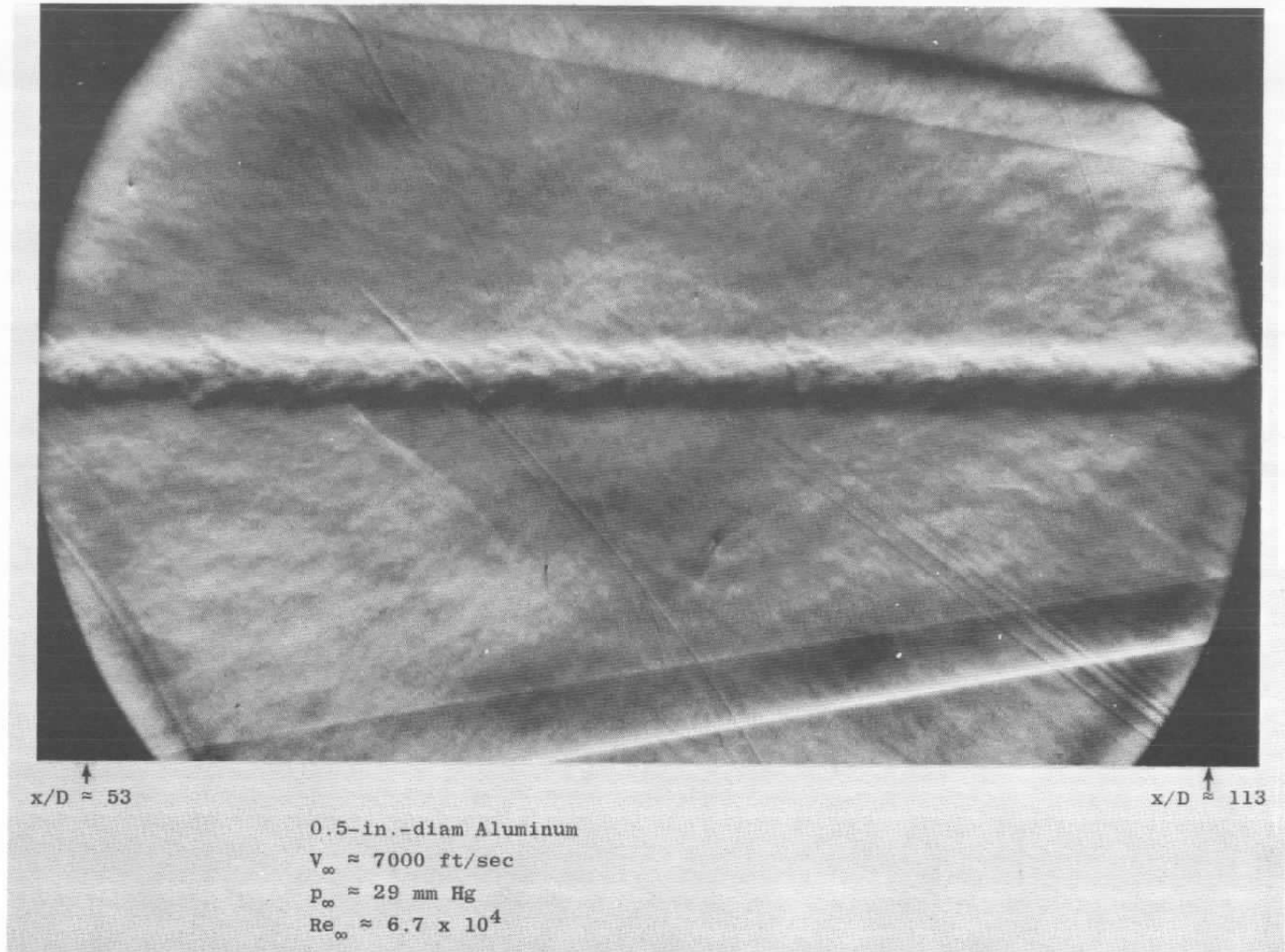
a. $V_{\infty} \approx 6.660$ ft/sec, $p_{\infty} \approx 14.7$ mm Hg, and $Re_{\infty} \approx 3.2 \times 10^4$

Fig. 7 Sphere Wake at Low Speed and Low Ambient Pressure



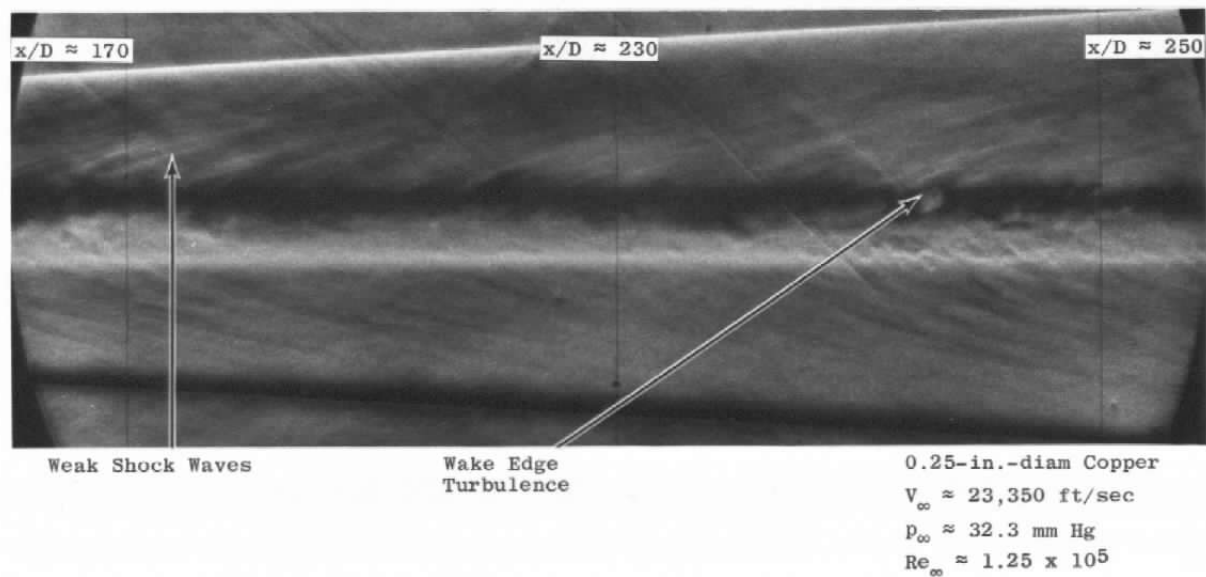
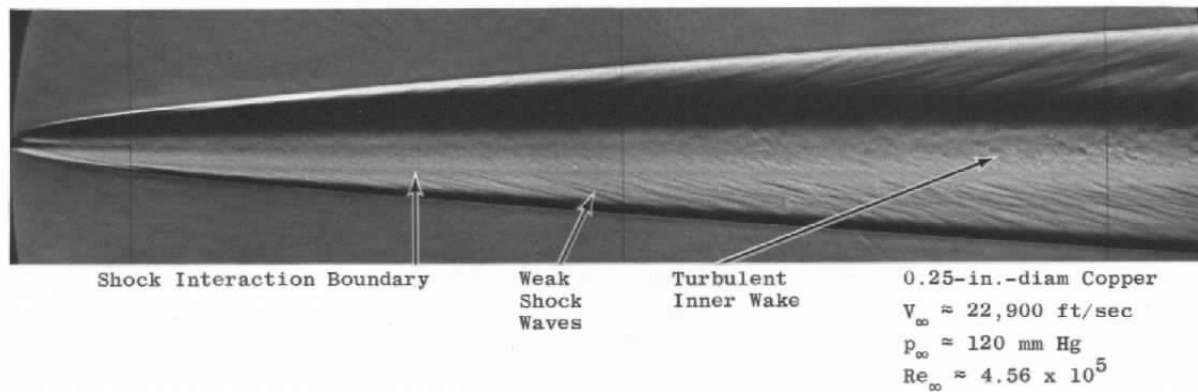
b. $V_\infty = 10,200$ ft/sec, $p_\infty = 10.3$ mm Hg, and $Re_\infty = 6.95 \times 10^4$

Fig. 7 Continued



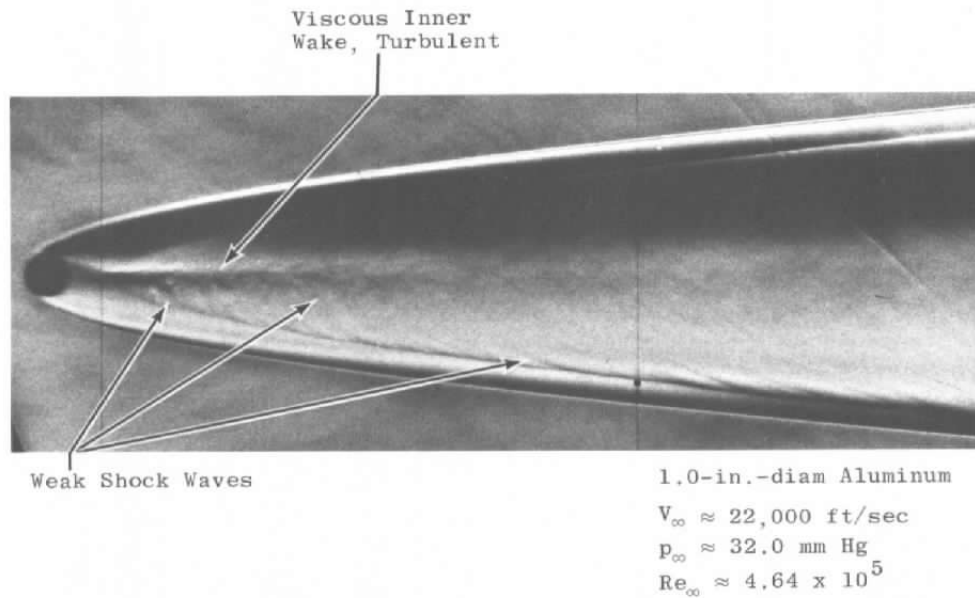
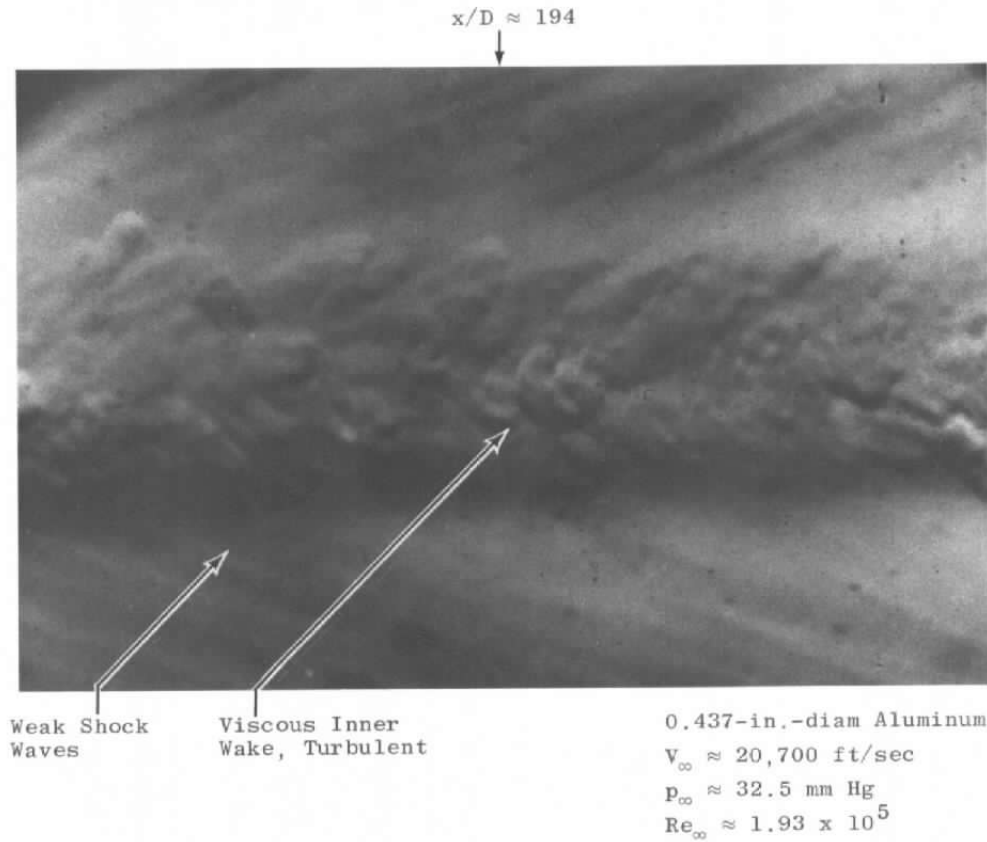
c. $V_\infty \approx 7000$ ft/sec, $p_\infty \approx 29$ mm Hg, and $Re_\infty \approx 6.7 \times 10^4$

Fig. 7 Concluded



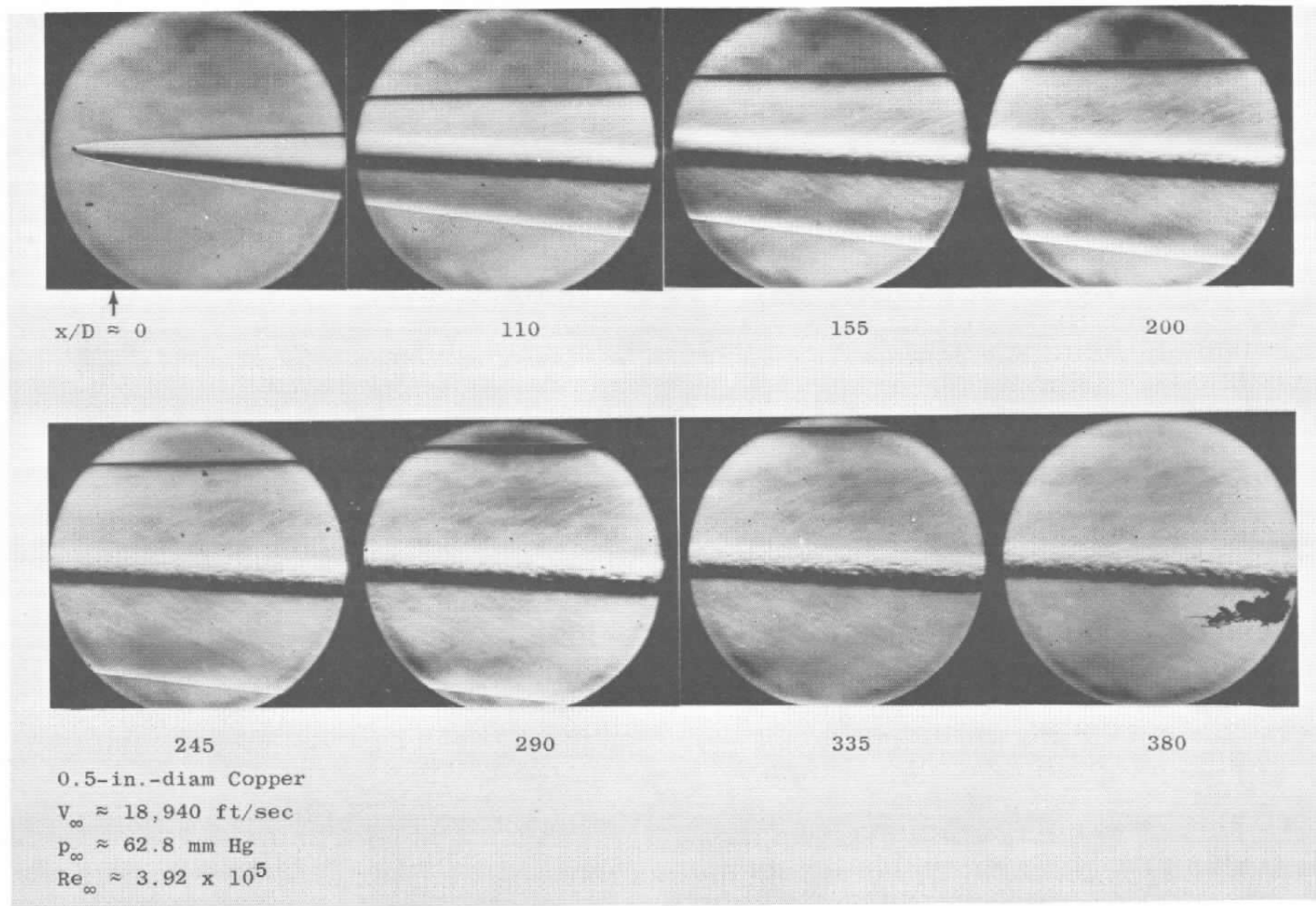
- a. $V_\infty \approx 22,900$ ft/sec, $p_\infty \approx 120$ mm Hg, and $Re_\infty \approx 4.56 \times 10^5$;
 $V_\infty \approx 23,350$ ft/sec, $p_\infty \approx 32.3$ mm Hg, and $Re_\infty \approx 1.25 \times 10^5$

Fig. 8 High-Speed Sphere Wake



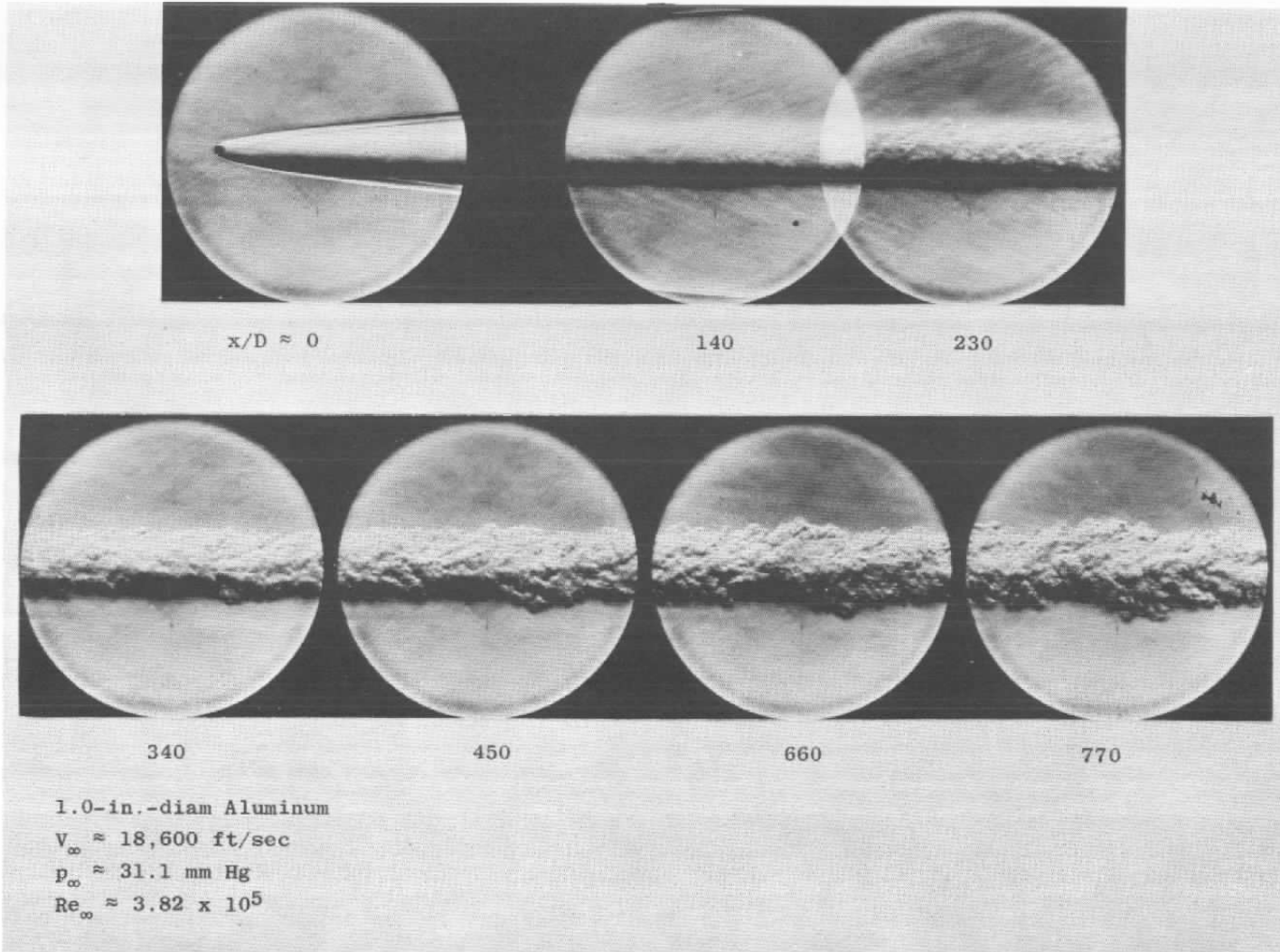
- b. $V_\infty \approx 20,700$ ft/sec, $p_\infty \approx 32.5$ mm Hg, and $Re_\infty \approx 1.93 \times 10^5$;
 $V_\infty \approx 22,000$ ft/sec, $p_\infty \approx 32.0$ mm Hg, and $Re_\infty \approx 4.64 \times 10^5$

Fig. 8 Concluded



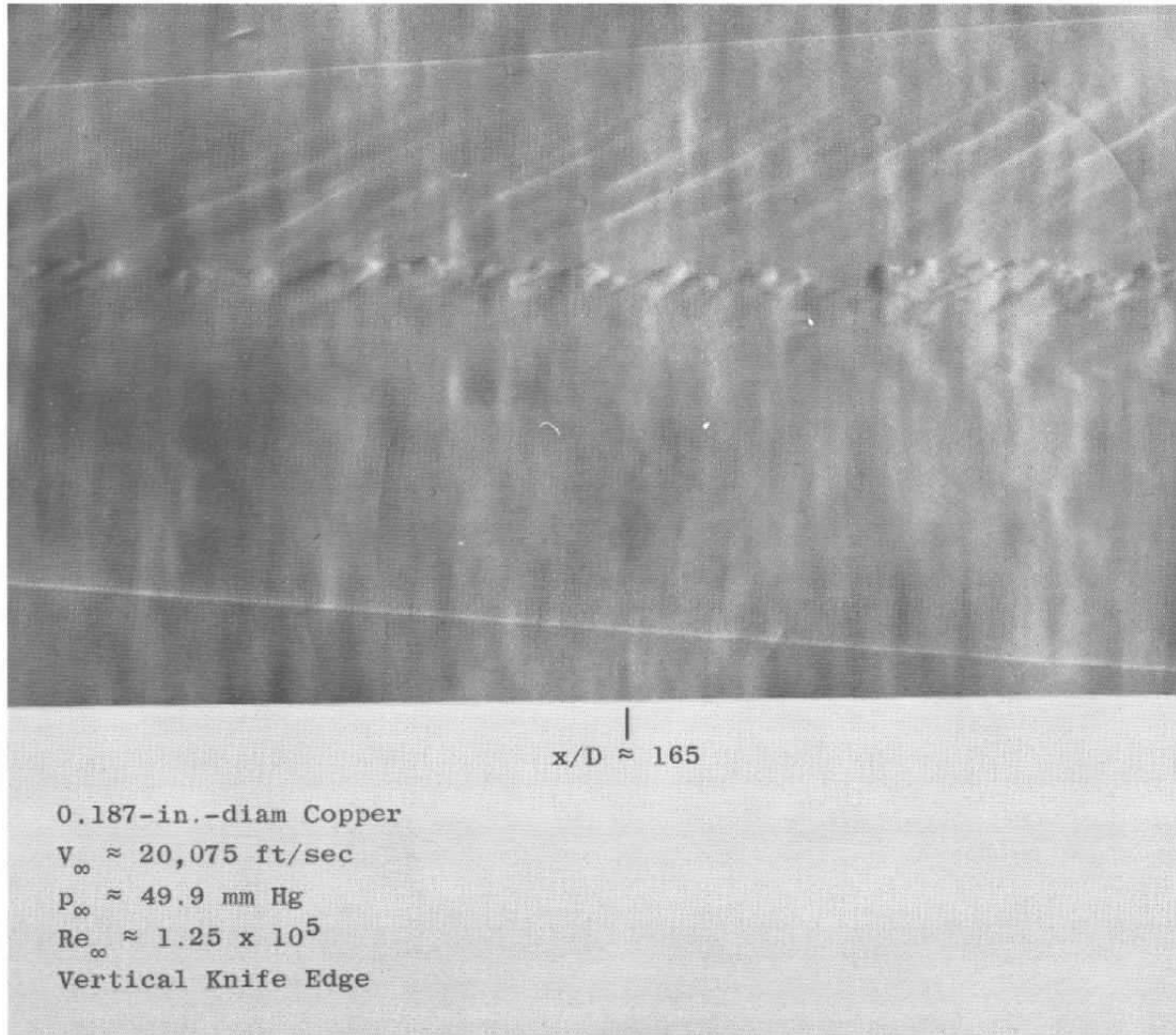
a. $V_\infty \approx 18,940$ ft/sec, $p_\infty = 62.8$ mm Hg, and $Re_\infty \approx 3.92 \times 10^5$

Fig. 9 High-Speed Breakthrough



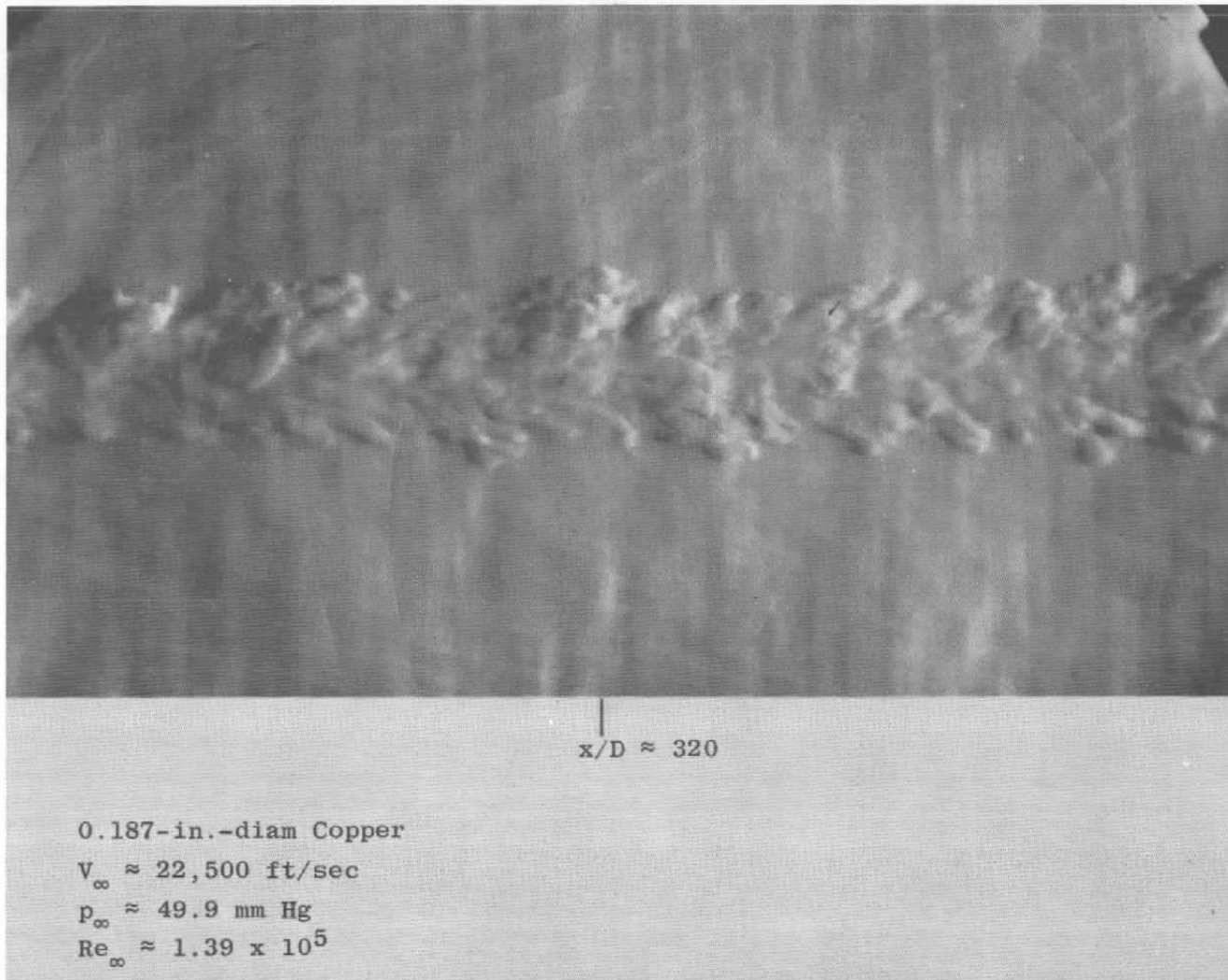
b. $V_\infty \approx 18,600$ ft/sec, $p_\infty \approx 31.1$ mm Hg, and $Re_\infty \approx 3.82 \times 10^5$

Fig. 9 Concluded



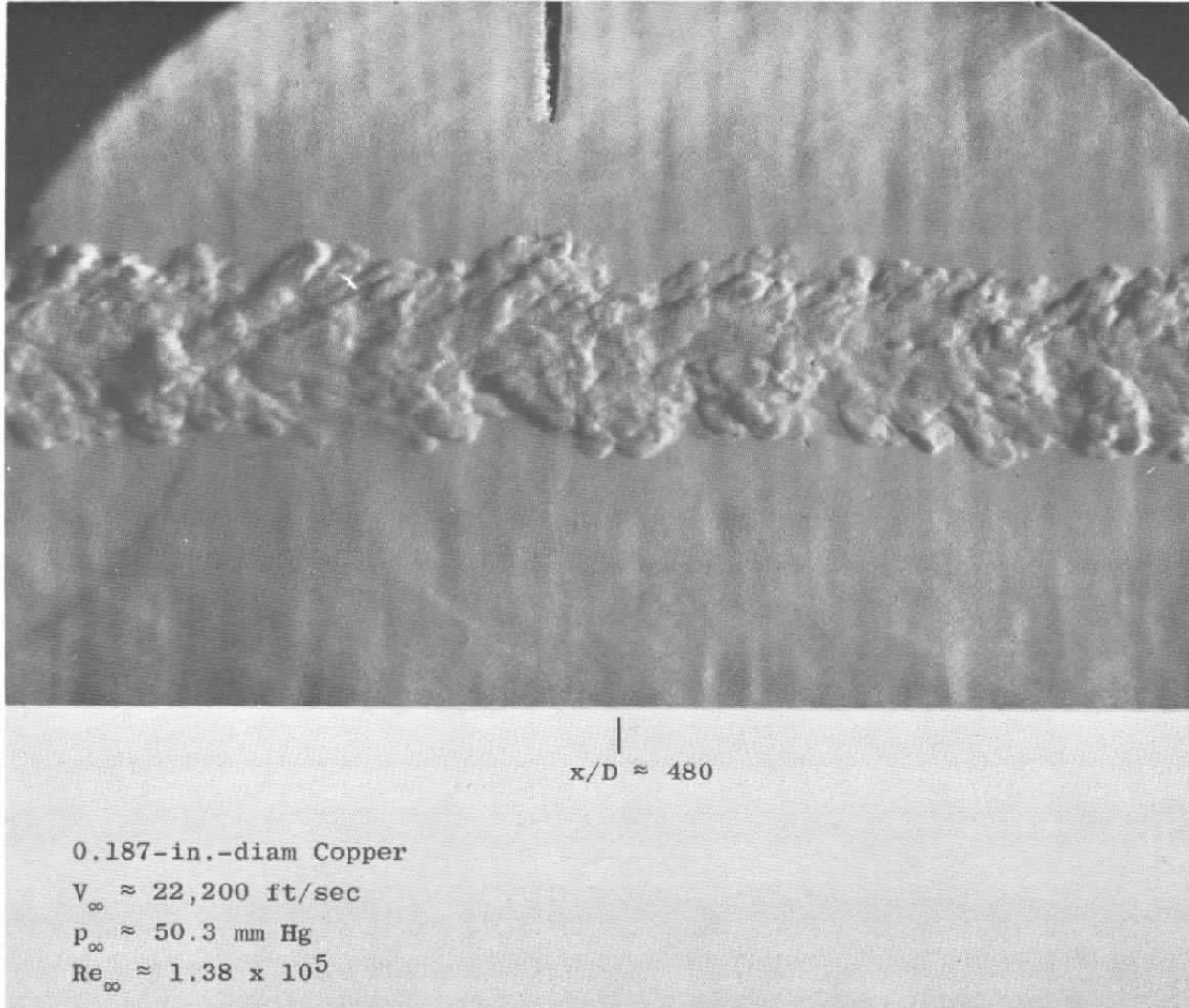
a. $V_\infty = 20,075$ ft/sec, $p_\infty = 49.9$ mm Hg, and $Re_\infty = 1.25 \times 10^5$

Fig. 10 High-Speed Turbulent Wake



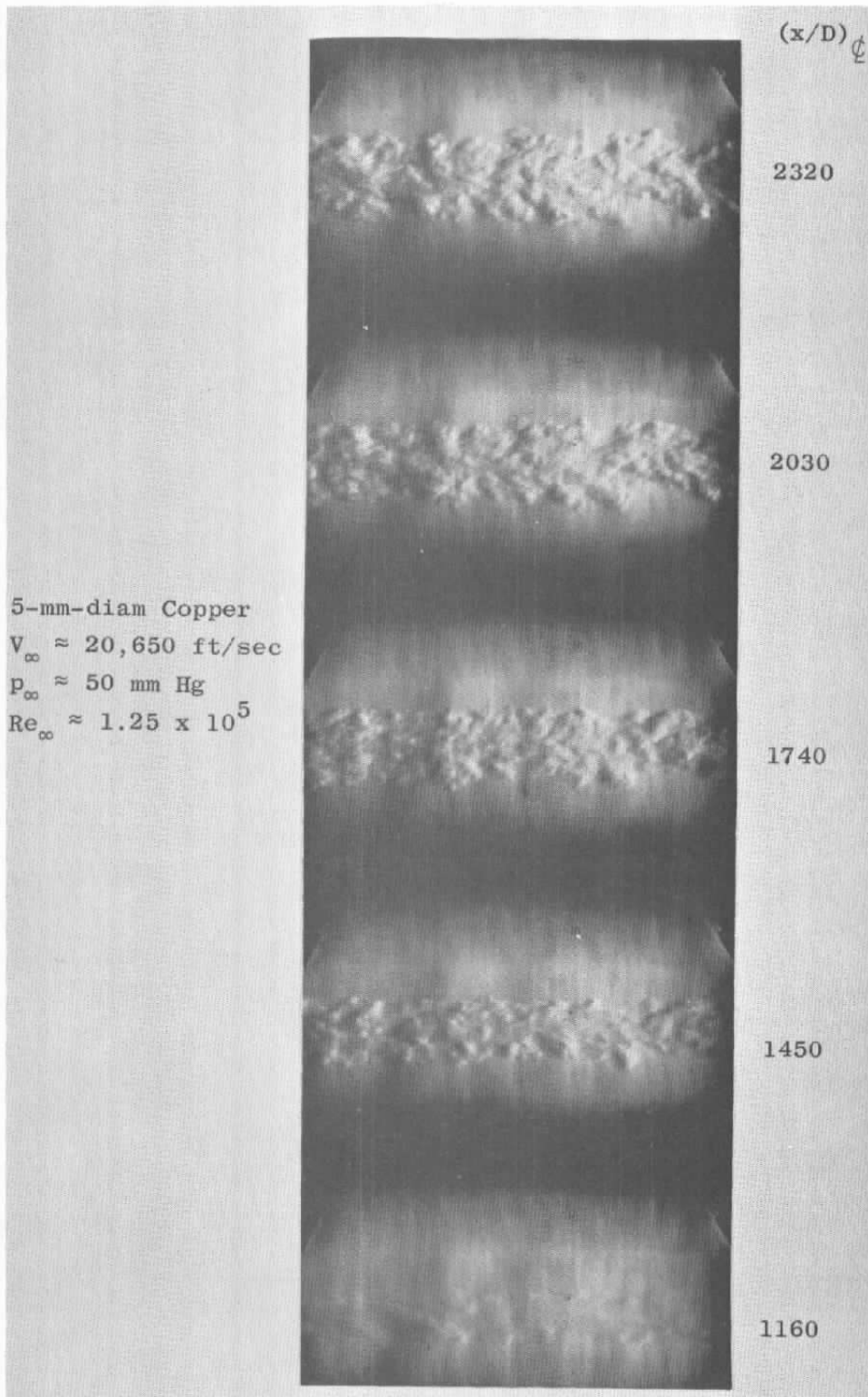
b. $V_\infty \approx 22,500$ ft/sec, $p_\infty = 49.9$ mm Hg, and $Re_\infty = 1.39 \times 10^5$

Fig. 10 Continued



c. $V_\infty = 22,200$ ft/sec, $p_\infty = 50.3$ mm Hg, and $Re_\infty = 1.38 \times 10^5$

Fig. 10 Continued



d. $V_{\infty} \approx 20,650$ ft/sec, $p_{\infty} \approx 50$ mm Hg, and $Re_{\infty} \approx 1.25 \times 10^5$

Fig. 10 Concluded

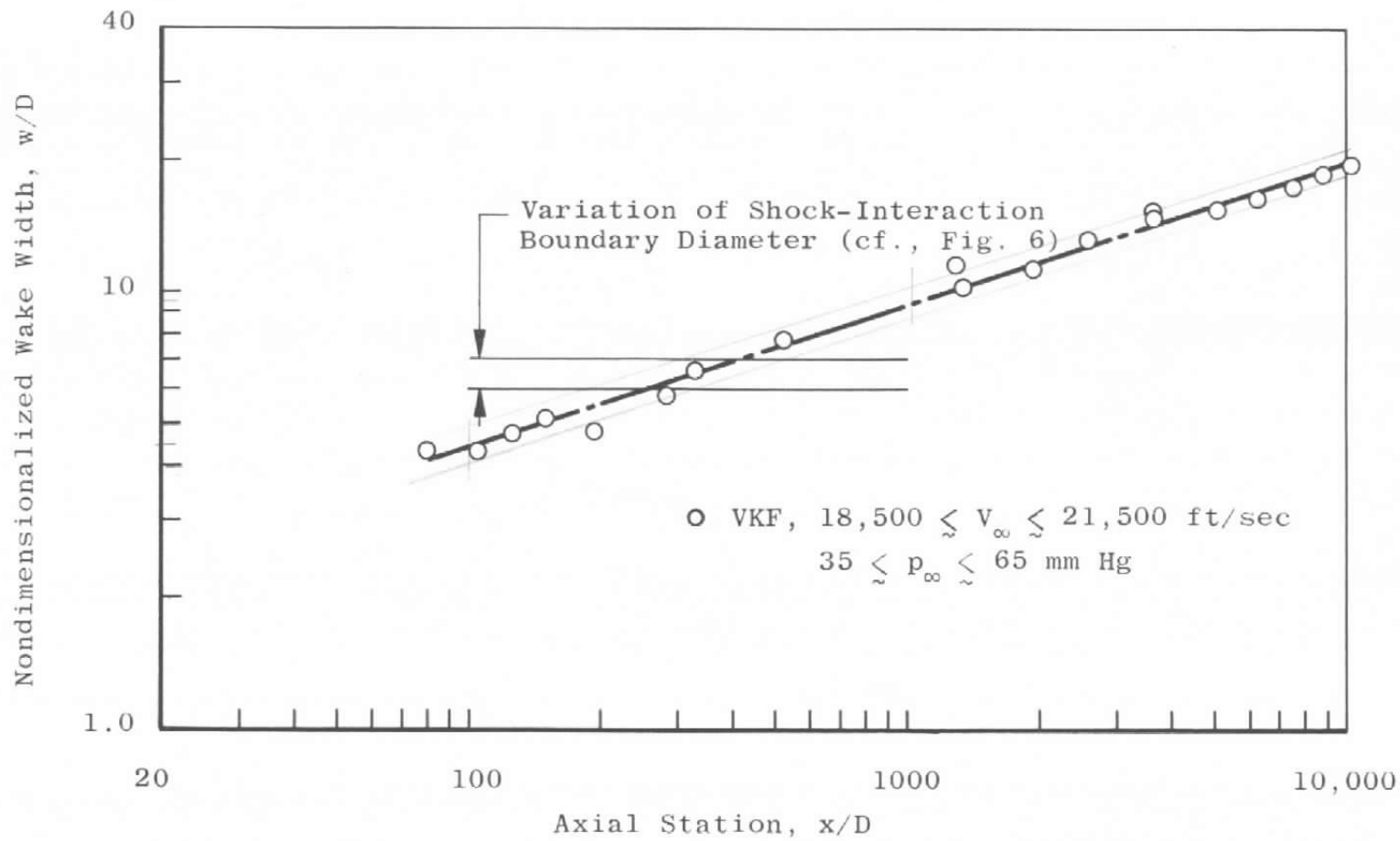


Fig. 11 Sphere Wake Diameter

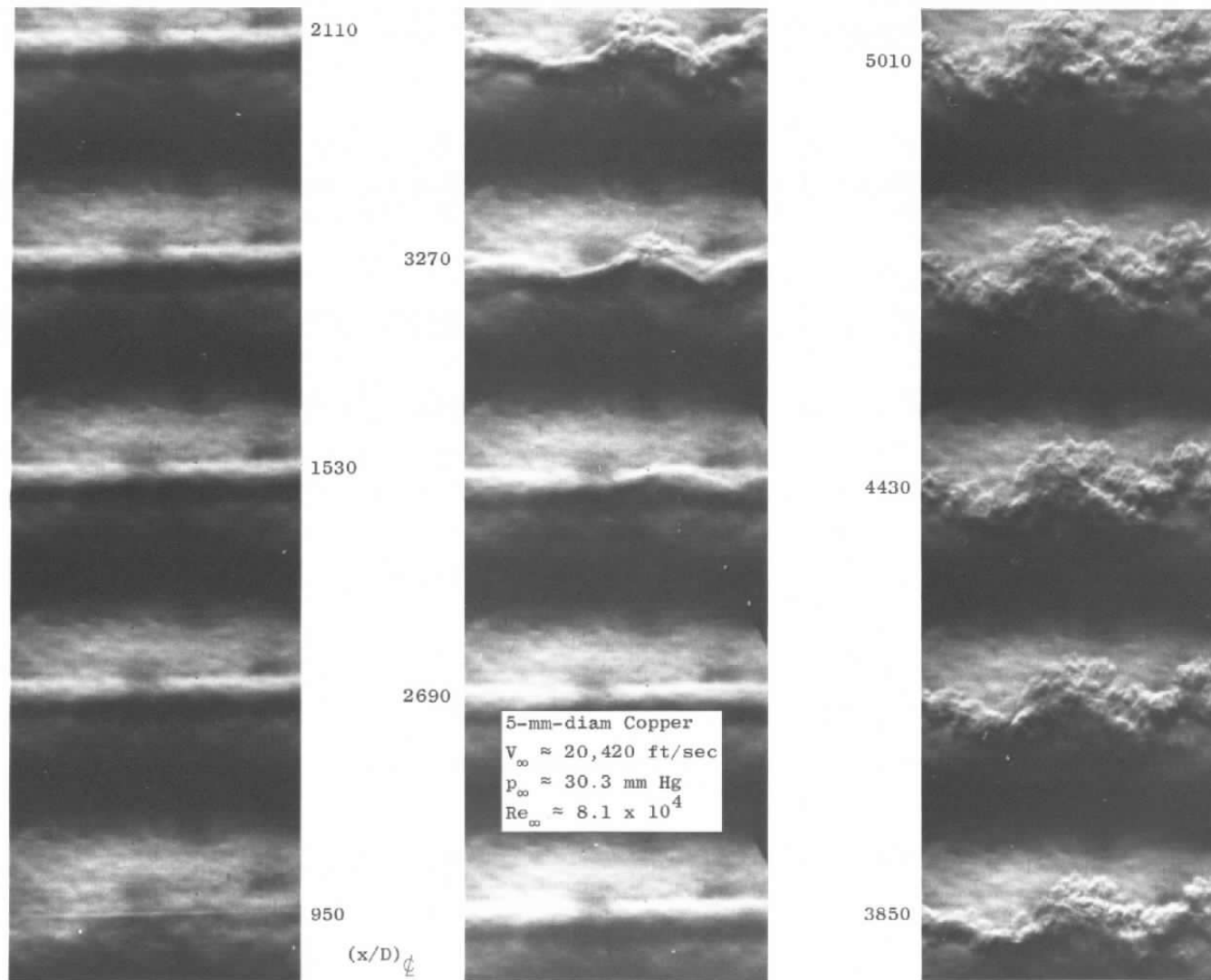


Fig. 12 Wake Characteristics at Low Reynolds Number

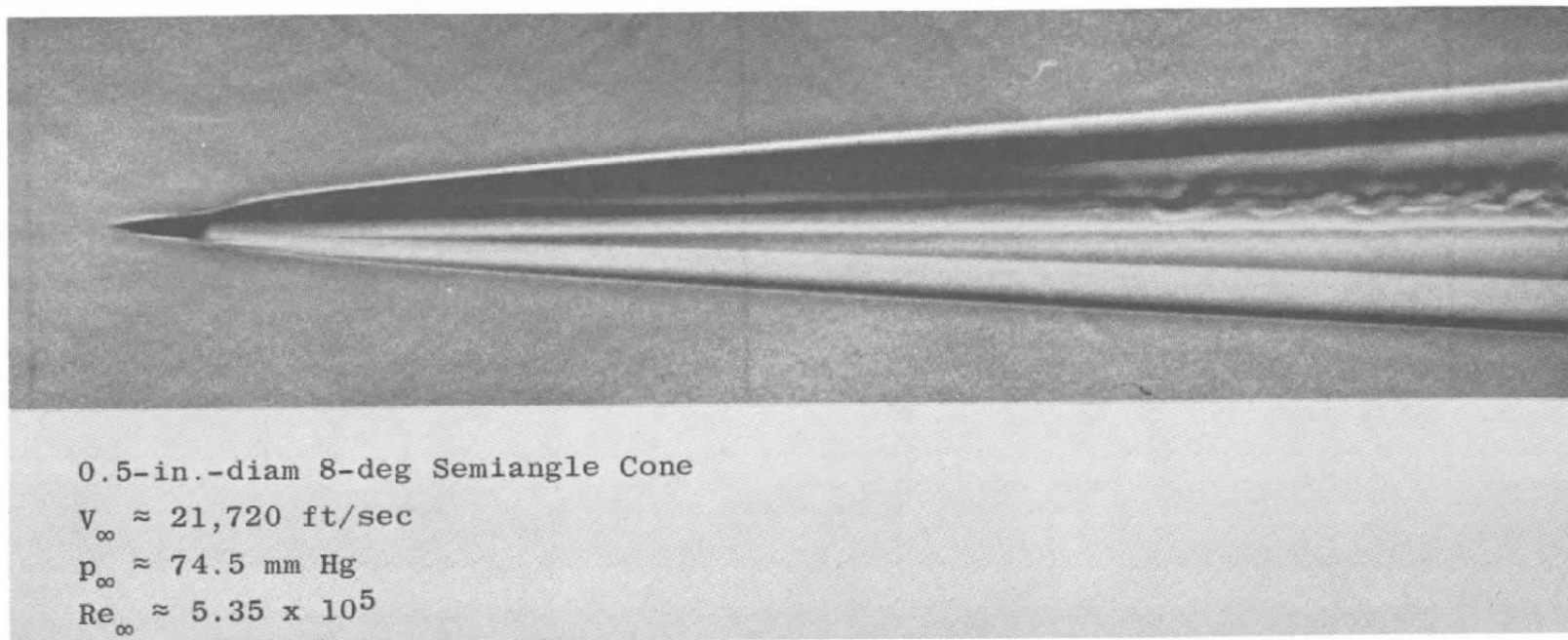
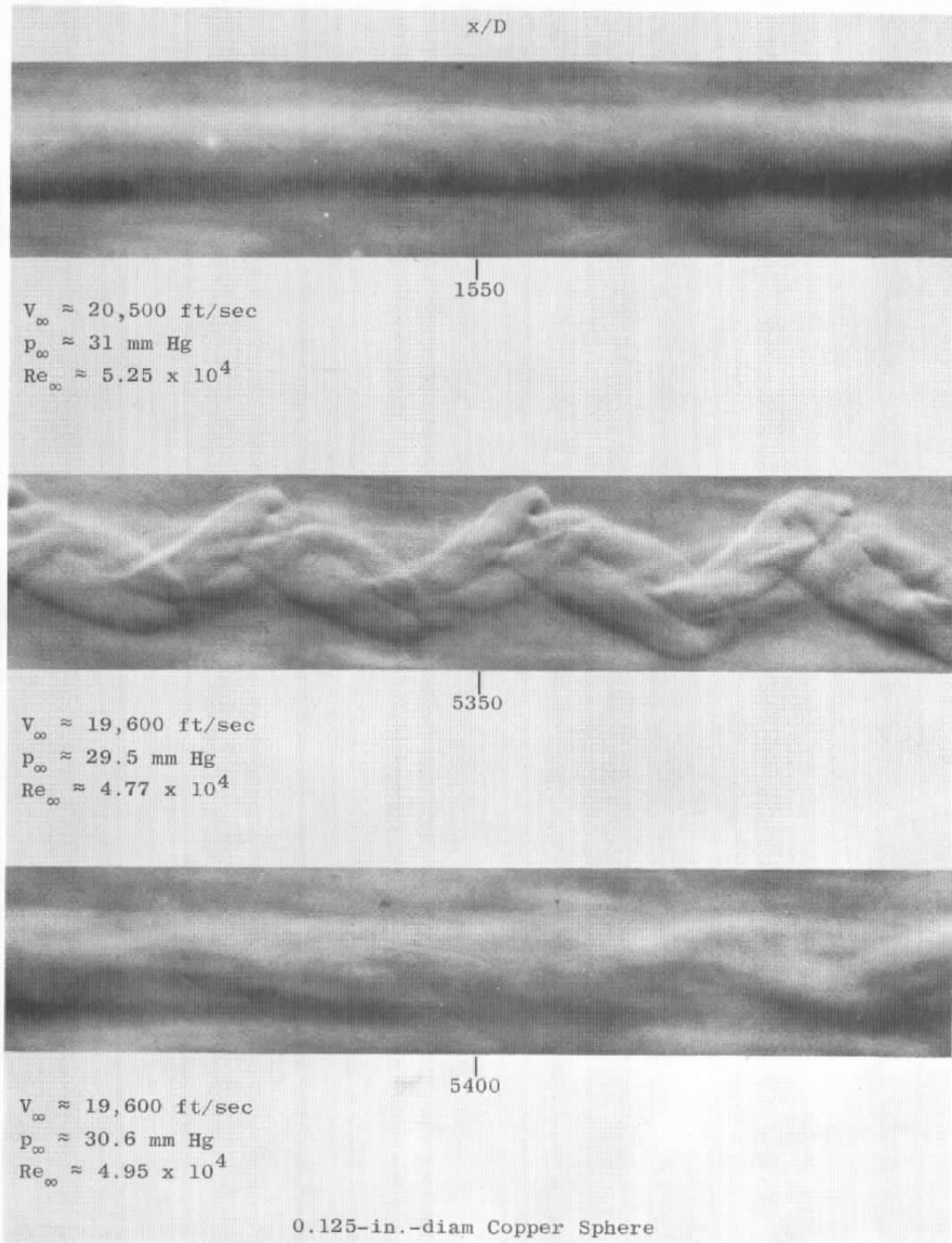
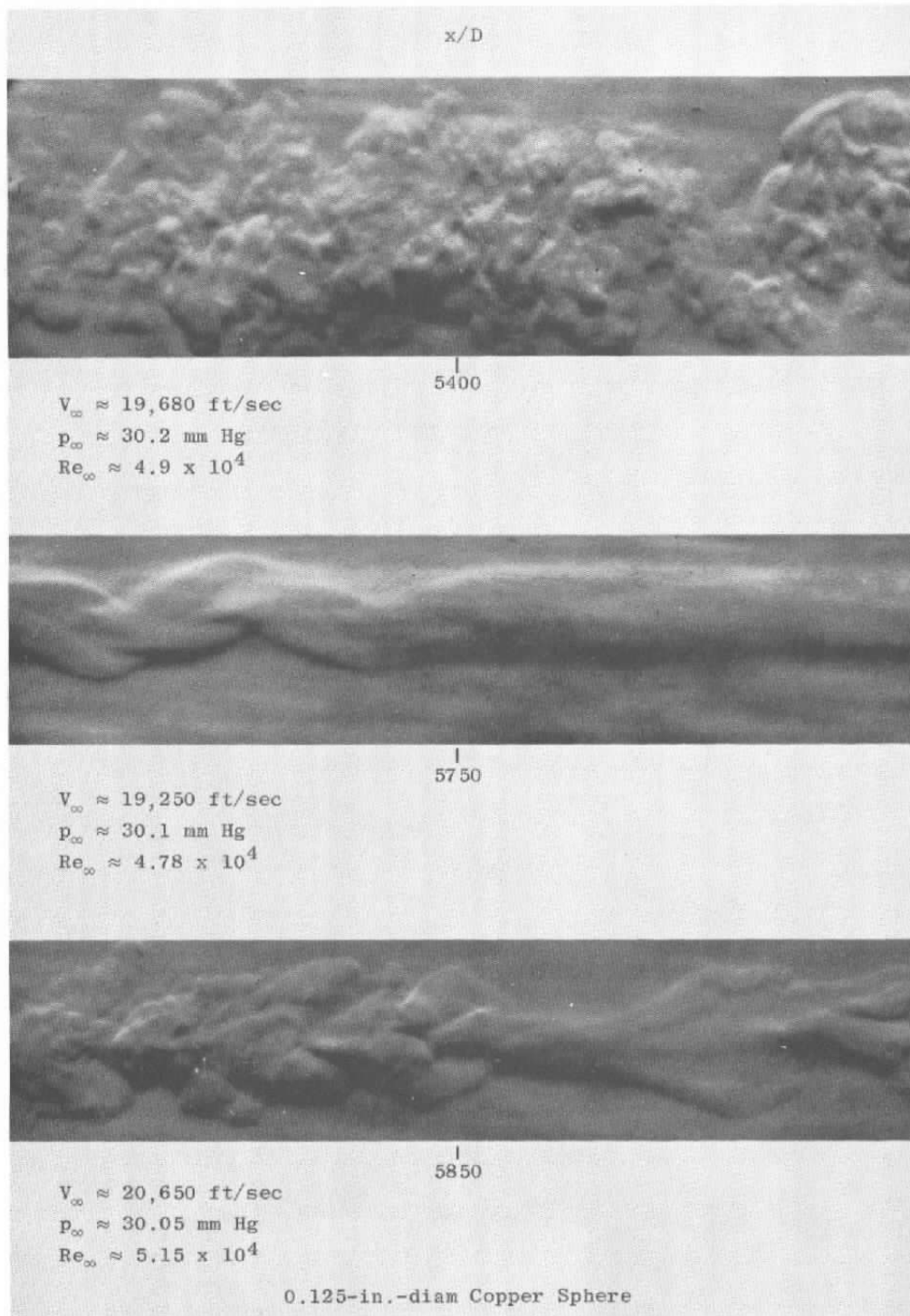


Fig. 13 Laminar Wake Breakup of a Hypersonic Slender Cone



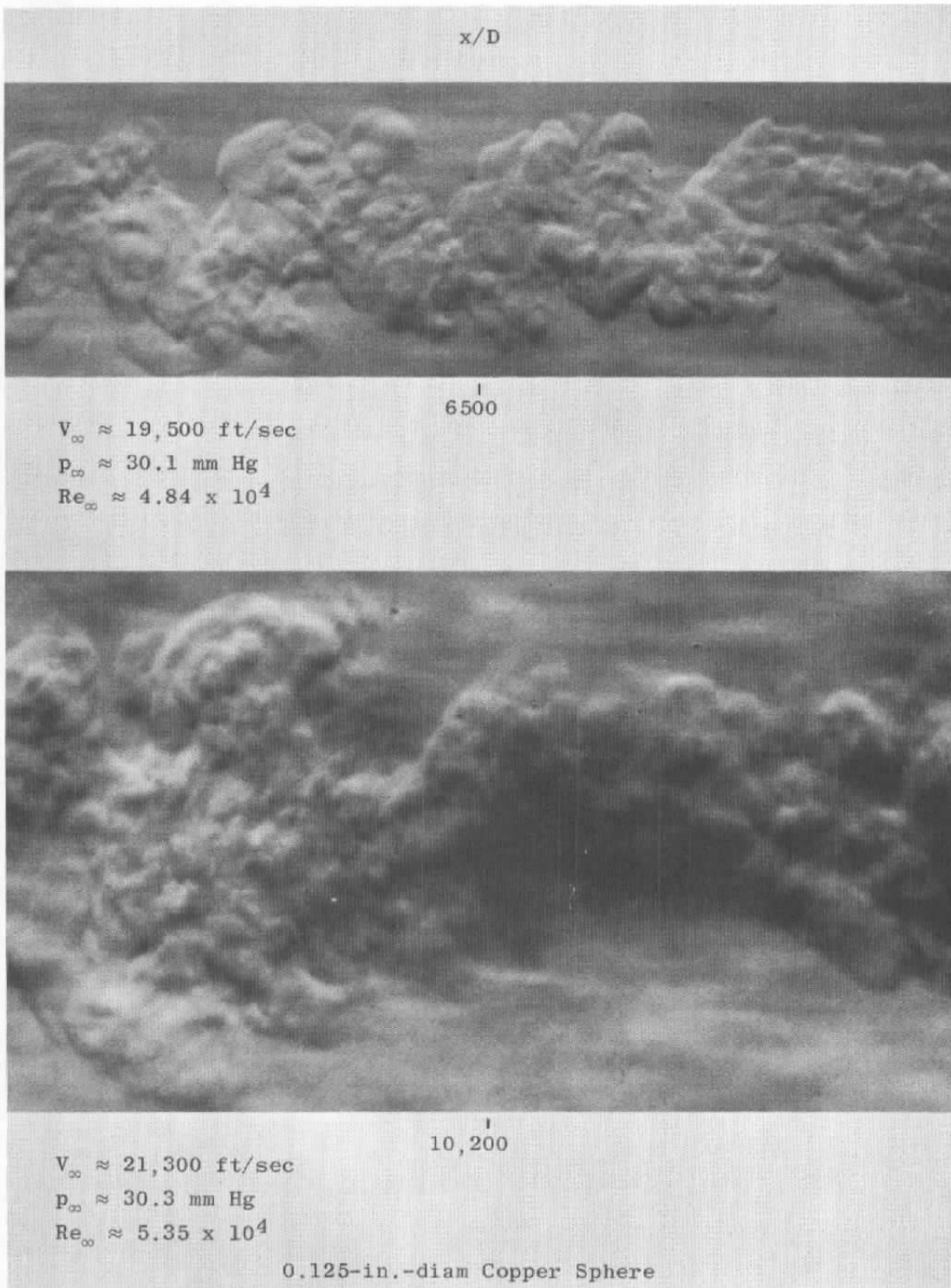
- a. $V_\infty \approx 20,500$ ft/sec, $p_\infty \approx 31$ mm Hg, and $Re_\infty \approx 5.25 \times 10^4$;
 $V_\infty \approx 19,600$ ft/sec, $p_\infty \approx 29.5$ mm Hg, and $Re_\infty \approx 4.77 \times 10^4$;
 $V_\infty \approx 19,600$ ft/sec, $p_\infty \approx 30.6$ mm Hg, and $Re_\infty \approx 4.95 \times 10^4$

Fig. 14 Wake Characteristics at Low Reynolds Number



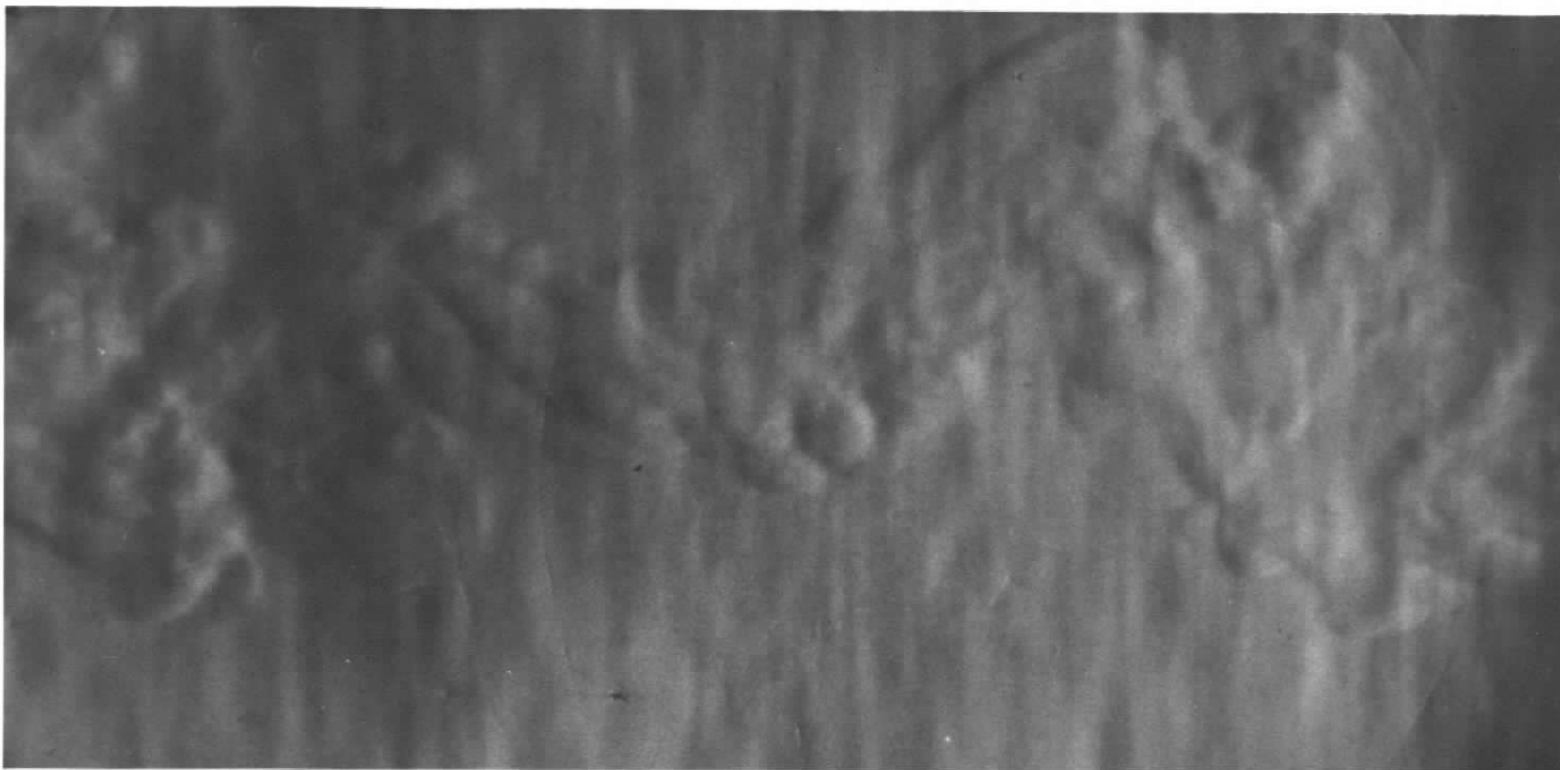
- b. $V_{\infty} \approx 19,680$ ft/sec, $p_{\infty} \approx 30.2$ mm Hg, and $Re_{\infty} \approx 4.9 \times 10^4$;
 $V_{\infty} \approx 19,250$ ft/sec, $p_{\infty} \approx 30.1$ mm Hg, and $Re_{\infty} \approx 4.78 \times 10^4$;
 $V_{\infty} \approx 20,650$ ft/sec, $p_{\infty} \approx 30.05$ mm Hg, and $Re_{\infty} \approx 5.15 \times 10^4$

Fig. 14 Continued



- c. $V_{\infty} \approx 19,500 \text{ ft/sec}$, $p_{\infty} \approx 30.1 \text{ mm Hg}$, and $Re_{\infty} \approx 4.84 \times 10^4$;
 $V_{\infty} \approx 21,300 \text{ ft/sec}$, $p_{\infty} \approx 30.3 \text{ mm Hg}$, and $Re_{\infty} \approx 5.35 \times 10^4$

Fig. 14 Continued



x/D \approx 6500

0.187-in.-diam Stainless Steel Sphere

$V_{\infty} \approx 20,250$ ft/sec

$p_{\infty} \approx 19.3$ mm Hg

$Re_{\infty} \approx 4.89 \times 10^4$

d. $V_{\infty} = 20,250$ ft/sec, $p_{\infty} = 19.3$ mm Hg, and $Re_{\infty} = 4.89 \times 10^4$

Fig. 14 Concluded

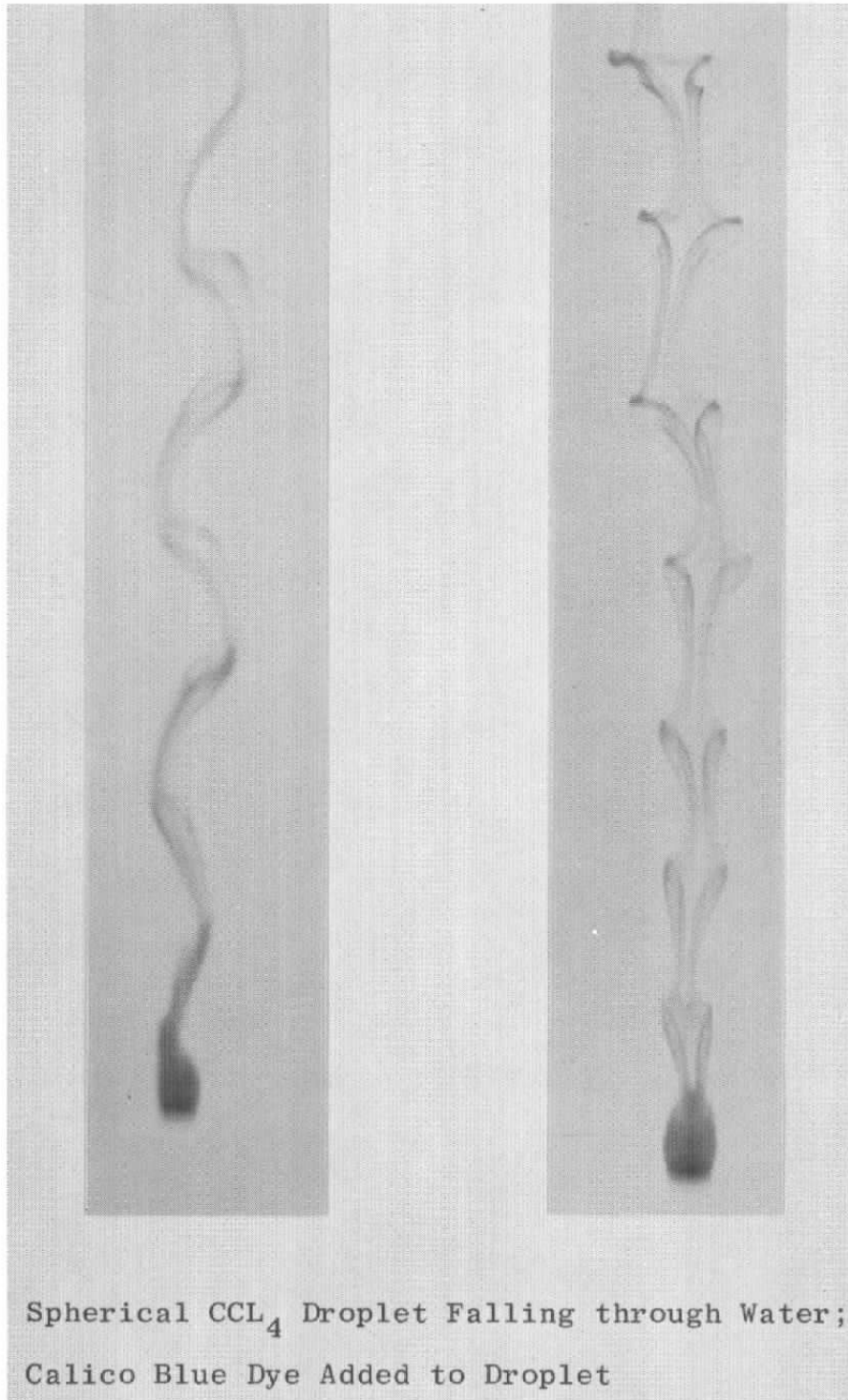
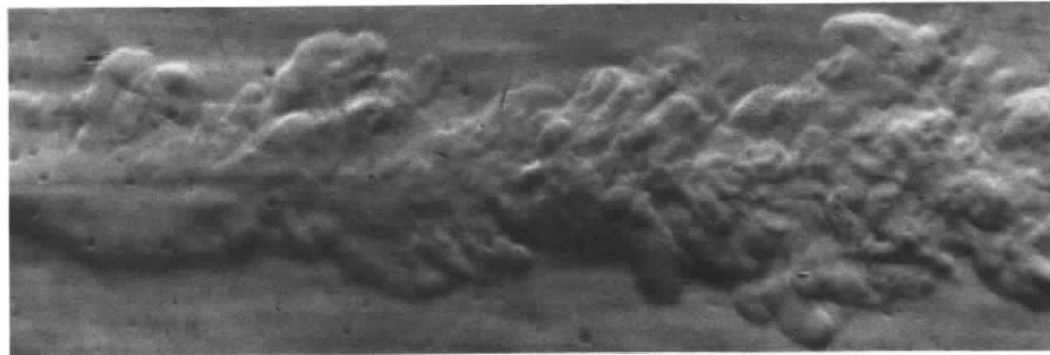


Fig. 15 Incompressible Wake of Bluff Body


 $x/D \approx 980$

0.25-in.-diam Aluminum
 $V_\infty \approx 21,450$ ft/sec
 $p_\infty \approx 19.85$ mm Hg
 $Re_\infty \approx 7.0 \times 10^4$


 $x/D \approx 1020$

0.25-in.-diam Copper
 $V_\infty \approx 21,150$ ft/sec
 $p_\infty \approx 21.15$ mm Hg
 $Re_\infty \approx 7.75 \times 10^4$

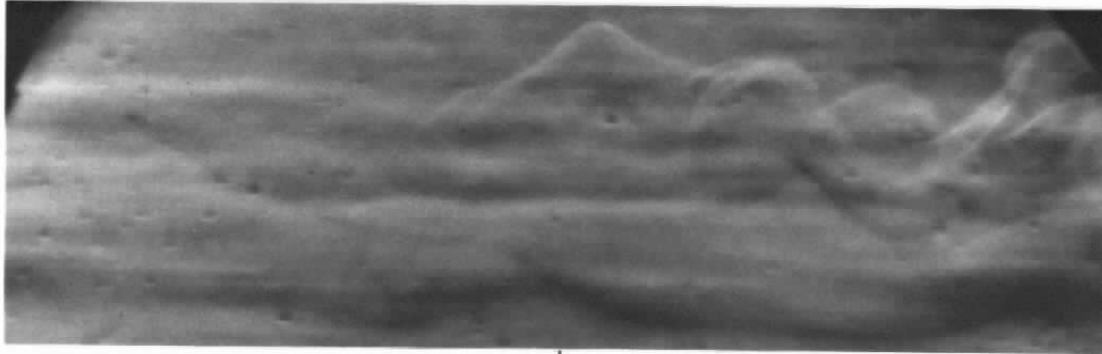
- a. $V_\infty \approx 21,450$ ft/sec, $p_\infty \approx 19.85$ mm Hg, and $Re_\infty \approx 7.0 \times 10^4$;
 $V_\infty \approx 21,150$ ft/sec, $p_\infty \approx 21.15$ mm Hg, and $Re_\infty \approx 7.75 \times 10^4$

Fig. 16 Far Wake Characteristics for Various Model Materials



$x/D \approx 1050$

0.25-in.-diam Nylon
 $V_\infty \approx 23,000$ ft/sec
 $p_\infty \approx 20.65$ mm Hg
 $Re_\infty \approx 7.8 \times 10^4$

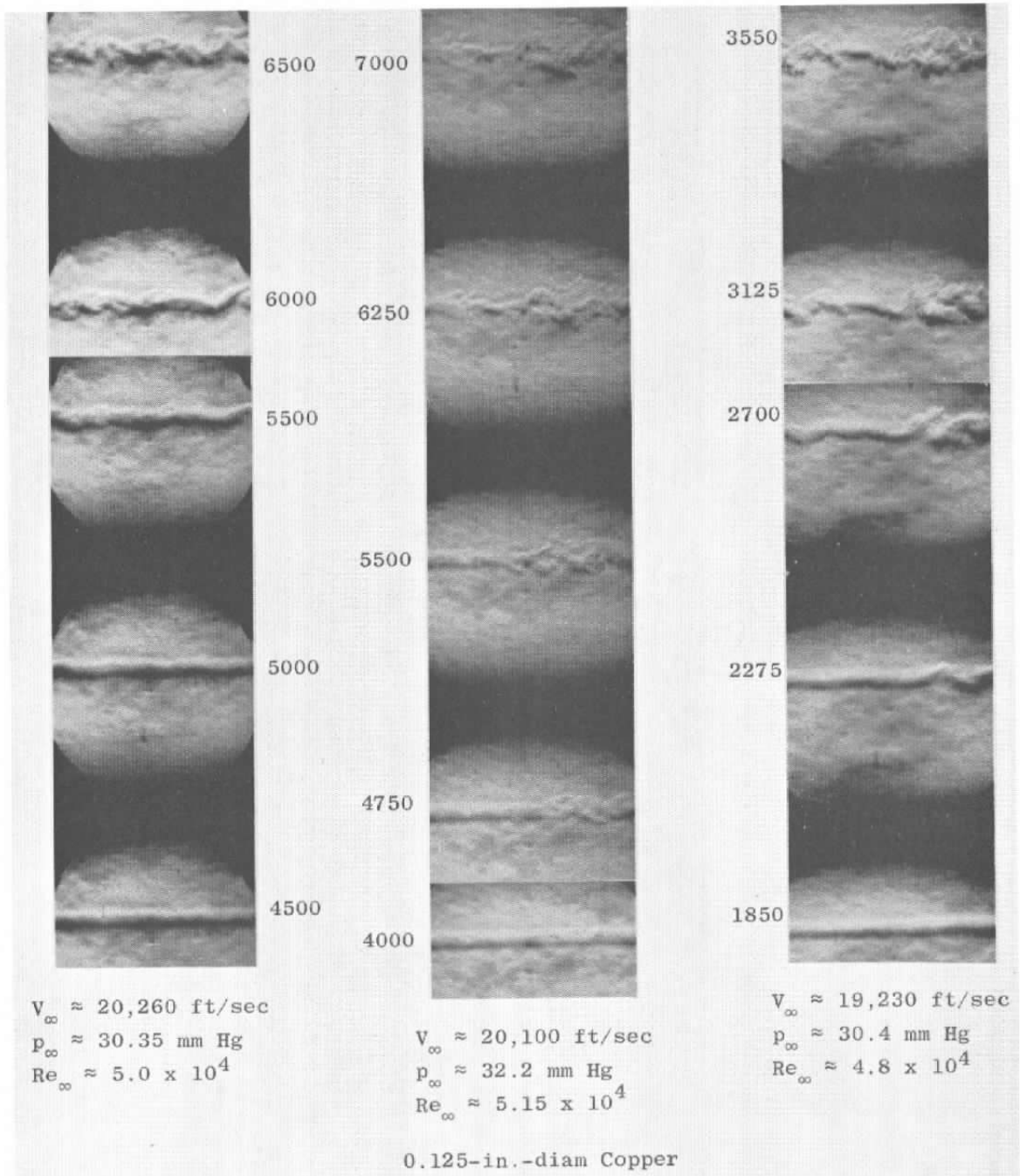


$x/D \approx 500$

0.25-in.-diam Nylon
 $V_\infty \approx 19,800$ ft/sec
 $p_\infty \approx 10$ mm Hg
 $Re_\infty \approx 3.3 \times 10^4$

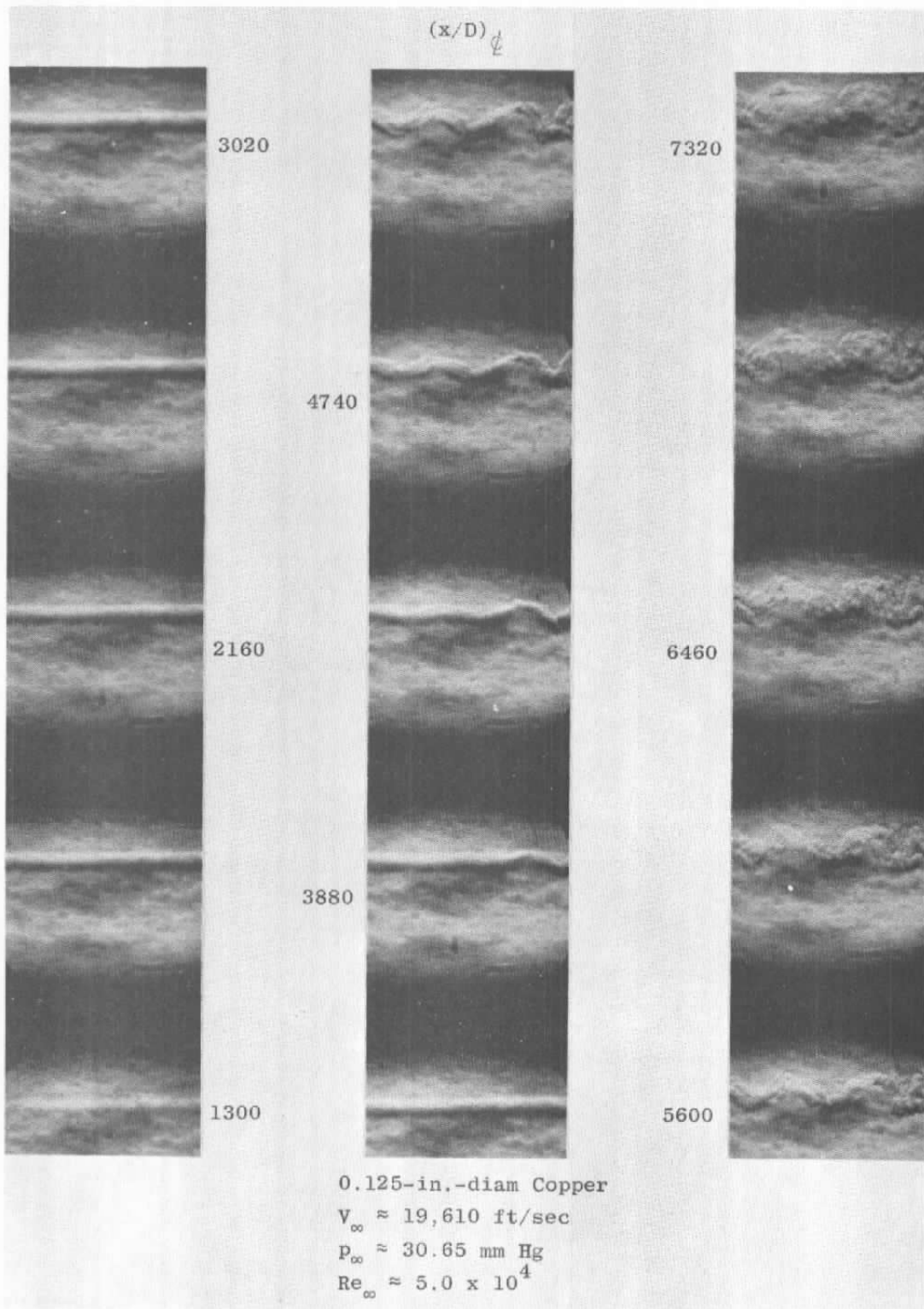
- b. $V_\infty \approx 23,000$ ft/sec, $p_\infty \approx 20.65$ mm Hg, and $Re_\infty \approx 7.8 \times 10^4$;
 $V_\infty \approx 19,800$ ft/sec, $p_\infty \approx 10$ mm Hg, and $Re_\infty \approx 3.3 \times 10^4$

Fig. 16 Concluded



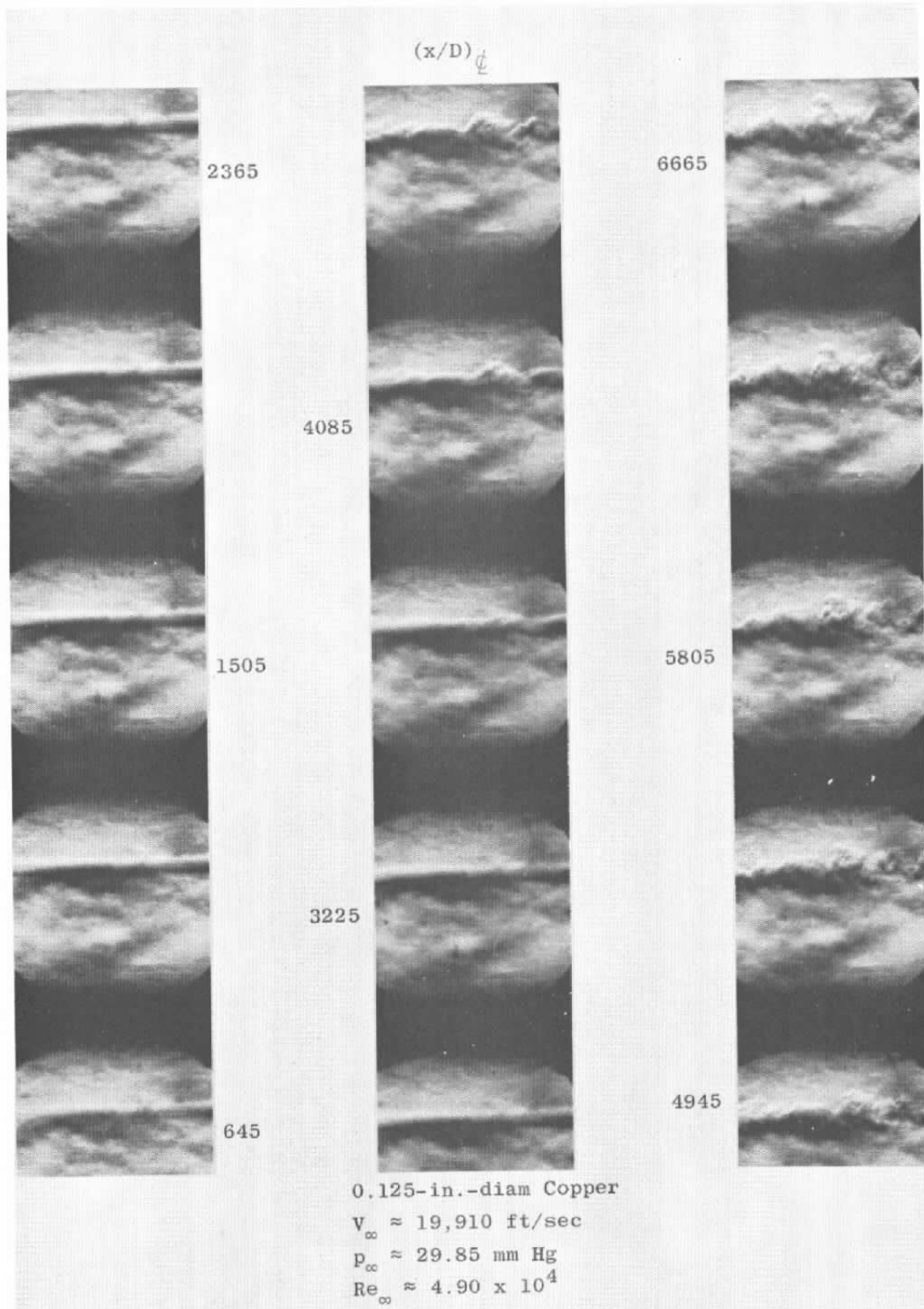
- a. $V_{\infty} = 20,260 \text{ ft/sec}$, $p_{\infty} = 30.35 \text{ mm Hg}$, and $Re_{\infty} = 5.0 \times 10^4$;
 $V_{\infty} = 20,100 \text{ ft/sec}$, $p_{\infty} = 32.2 \text{ mm Hg}$, and $Re_{\infty} = 5.15 \times 10^4$;
 $V_{\infty} = 19,230 \text{ ft/sec}$, $p_{\infty} = 30.4 \text{ mm Hg}$, and $Re_{\infty} = 4.8 \times 10^4$

Fig. 17 High-Speed, Low Reynolds Number Sphere Wake



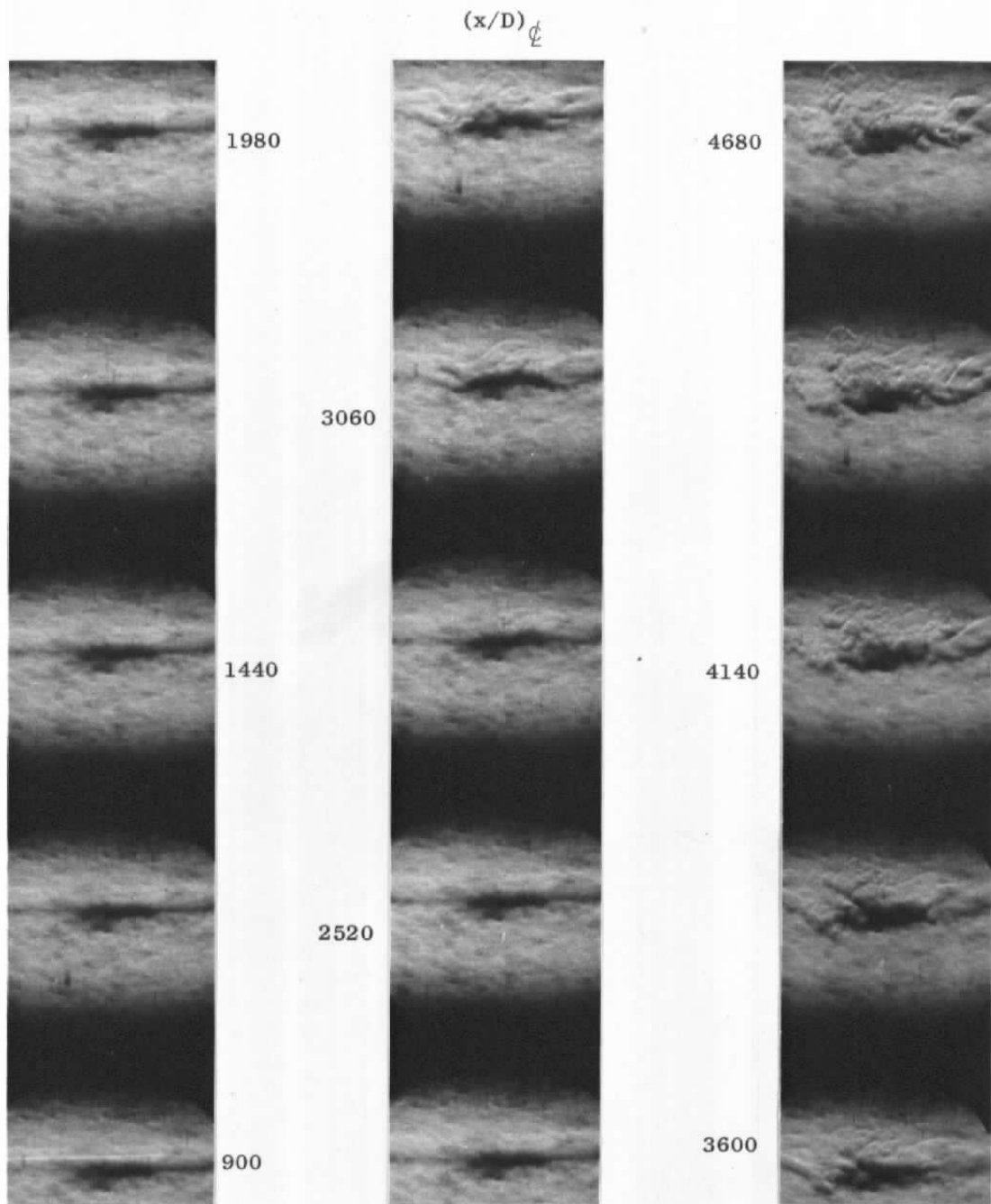
b. $V_\infty \approx 19,610$ ft/sec, $p_\infty \approx 30.65$ mm Hg, and $Re_\infty \approx 5.0 \times 10^4$

Fig. 17 Continued



c. $V_\infty \approx 19,910$ ft/sec, $p_\infty \approx 29.85$ mm Hg, and $Re_\infty \approx 4.90 \times 10^4$

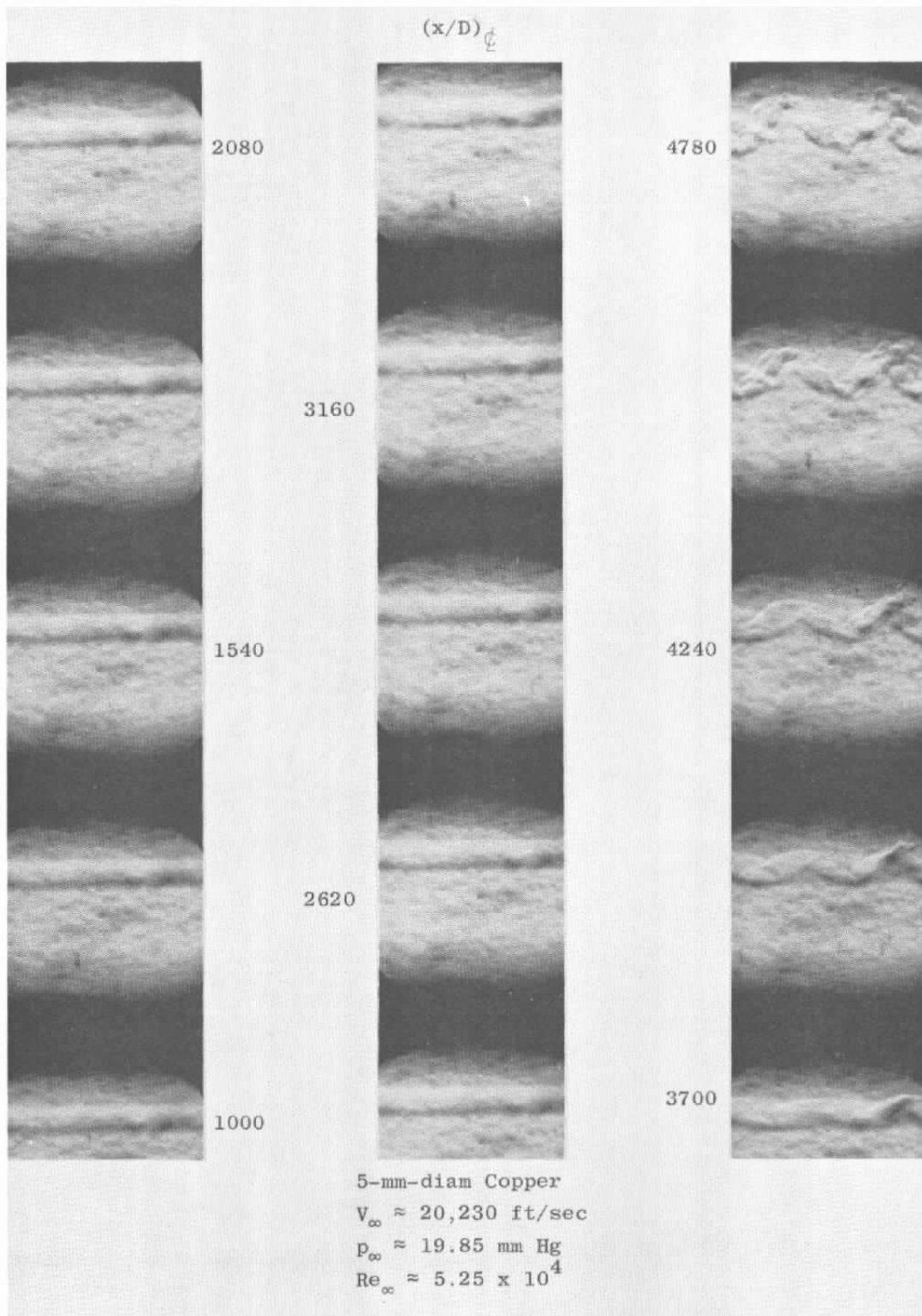
Fig. 17 Continued



5-mm-diam Copper
 $V_\infty \approx 20,440$ ft/sec
 $p_\infty \approx 20$ mm Hg
 $Re_\infty \approx 5.35 \times 10^4$

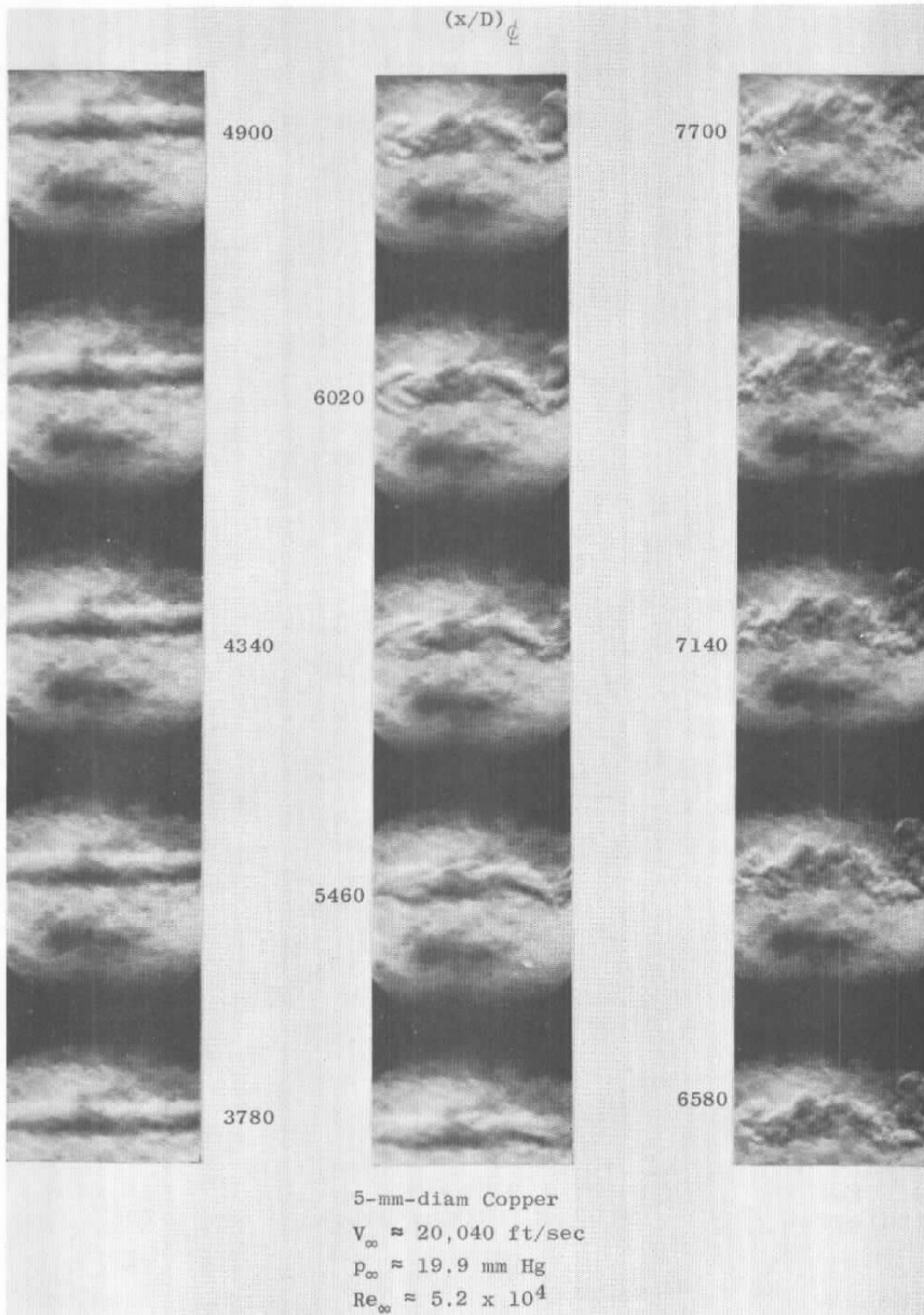
d. $V_\infty \approx 20,440$ ft/sec, $p_\infty \approx 20$ mm Hg, and $Re_\infty \approx 5.35 \times 10^4$

Fig. 17 Continued



e. $V_\infty \approx 20,230$ ft/sec, $p_\infty \approx 19.85$ mm Hg, and $Re_\infty \approx 5.25 \times 10^4$

Fig. 17 Continued



f. $V_\infty \approx 20,040$ ft/sec, $p_\infty \approx 19.9$ mm Hg, and $Re_\infty \approx 5.2 \times 10^4$

Fig. 17 Concluded

DOCUMENT CONTROL DATA - R & D

(Security classification of title, body of abstract and indexing annotation must be entered when the overall report is classified)

1. ORIGINATING ACTIVITY (Corporate author) Arnold Engineering Development Center ARO, Inc., Operating Contractor Arnold Air Force Station, Tennessee		2a. REPORT SECURITY CLASSIFICATION UNCLASSIFIED	
		2b. GROUP N/A	
3. REPORT TITLE OBSERVATIONS OF SPHERE WAKES OVER A WIDE RANGE OF VELOCITIES AND AMBIENT PRESSURES			
4. DESCRIPTIVE NOTES (Type of report and inclusive dates) January 1965 to March 1968 - Final Report			
5. AUTHOR(S) (First name, middle initial, last name) A. B. Bailey, ARO, Inc.			
6. REPORT DATE September 1968	7a. TOTAL NO OF PAGES 78	7b. NO OF REFS 18	
8a. CONTRACT OR GRANT NO F40600-69-C-0001 b. Program Element 6240533F c. 8952 d.		9a. ORIGINATOR'S REPORT NUMBER(S) AEDC-TR-68-112	
		9b. OTHER REPORT NO(S) (Any other numbers that may be assigned this report) N/A	
10. DISTRIBUTION STATEMENT This document is subject to special export controls and each transmittal to foreign governments or foreign nationals may be made only with prior approval of Arnold Engineering Development Center (AETS), Arnold Air Force Station, Tennessee 37389.			
11. SUPPLEMENTARY NOTES Available in DDC.		12. SPONSORING MILITARY ACTIVITY Arnold Engineering Development Center (AETS), Arnold AF Station, Tennessee 37389	
13. ABSTRACT The behavior of the near and far wake of spheres for a wide range of velocities, $4000 \leq V_{\infty} \leq 23,000$ ft/sec, and ambient pressures, $10 \leq p_{\infty} \leq 730$ mm Hg, has been studied with schlieren techniques in an aeroballistic free-flight range. In the present report, attention is drawn to some of the problems of interpreting photographs of this type. It is shown that the mode of operation of the schlieren system, e.g., vertical or horizontal knife edge, can exercise a profound effect on the aspects of the flow that are visualized. The breakthrough phenomenon, which has been considered to exist only at near reentry velocities, is shown to exist at lower supersonic speeds. Schlieren photographs of the far wake of hypersonic spheres in the Reynolds number range of $3 \times 10^4 \leq Re_{\infty} \leq 8 \times 10^4$ bear a marked resemblance to photographs of the wake of a subsonic bluff body. For both hypersonic and subsonic cases, this photographic evidence indicates the existence of a large-scale vortex structure in the wake. This document is subject to special export controls and each transmittal to foreign governments or foreign nationals may be made only with prior approval of Arnold Engineering Development Center (AETS), Arnold Air Force Station, Tennessee 37389.			

14	KEY WORDS	LINK A		LINK B		LINK C	
		ROLE	WT	ROLE	WT	ROLE	WT
	spheres near wakes far wakes free flight schlieren techniques interpretation problems breakthrough phenomenon						